A PhD Thesis in Physics

# The QCD Strong Coupling from Hadronic τ Decays

Dirk Hornung

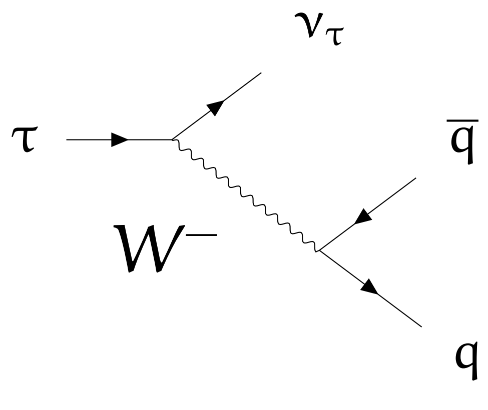


July 2019

Supervisors: Matthias Jamin, Santiago Peris Rodríguez

# Abstract

# Acknowledgements

# Notations

Abbreviations are given in small-caps. E.g sm instead of SM (following [**Boito2011**]).

Every abbreviation is indexed at the end of this thesis.

Important formulas are emphasised by a grey background (like in [**Schwartz2013**]).

Chapter 1

# Introduction

In particle physics we are concerned about small objects and their interactions. The smallest of these objects are referred to as *elemental particles*. Their dynamics are governed by the laws of nature. These laws are organised through symmetries, which are currently best described by the *Standard Model* (SM).

The SM classifies all known elementary particles and describes three of the four fundamental forces: the electromagnetic, weak and strong force. The particles representing matter are contained in two groups of fermionic, spin-1/2 particles. The former group, the leptons consist of: the electron ($e$), the muon ($\mu$), the tau ($\tau$) and their corresponding neutrinos $\nu_e$, $\nu_\mu$ and $\nu_\tau$. The latter group, the quarks contain: $u$, $d$ (up and down, the so called light quarks ), $s$ (strange), $c$ (charm), $b$ (bottom or beauty) and $t$ (top or truth). The three fundamental forces, the SM differentiates, are described through their carrier particles, the so-called bosons: the photon for the electromagnetic, the $Z$-or $W$-Boson for the weak and the gluon ($g$) for the strong interaction. and strong ($g$ gluon) interactions. The before mentioned Leptons solely interact through the electromagnetic and the weak force (also referred to as electroweak interaction), whereas the quarks additionally interact through the strong force. A short summary of the taxonomy of the SM can be seen in **??**

From a more mathematical point of view the SM is a gauge *Quantum Field Theory* (QFT). is the combination of *classical field theory*, *special relativity* and *quantum mechanics*. Its fundamental objects are ruled through its gauge-group $SU(3) \times SU(2) \times U(1)$. Each of its subgroups introduces a global and a local gauge symmetry. The global symmetry introduces the charges, which the

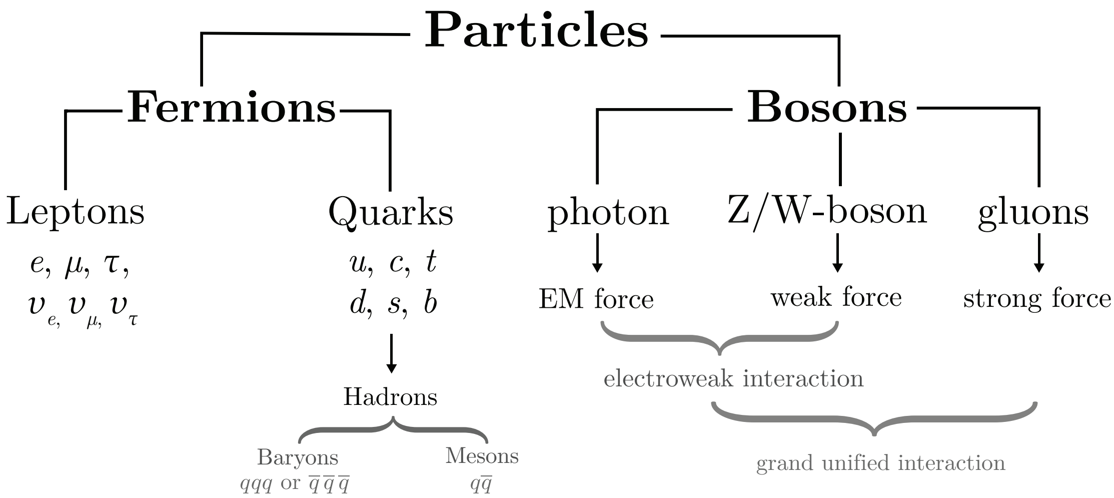


Figure 1.1: Taxonomy of the Standard Model.

fields are carrying. The local symmetry introduce the gauge-fields, which represent the previously mentioned force carriers. Naively every subgroup[1] of the gauge-group of the standard model is responsible for one of the three forces:

**U(1)** the *abelian* gauge group governs the representation of *quantum electrodynamics* (QED), which is commonly known as the electric force. Its global and local symmetry introduces the electric charge and the photon-field.

**SU(2)** Is the *non-abelian* symmetry group responsible for the weak-interaction. It introduces the $W^+, W^-$ and Z bosons and the weak charge. The gauge groups U(1) and SU(2) have been combined to the *electroweak interaction*.

**SU(3)** The SU(3)-group is also *non-abelian* and governs the strong interactions, which are summarised in the theory of *Quantum Chromodynamics* (QCD). The group yields the three colour charges and due to its eight-dimensional adjoint-representation, eight different gluons.

Unfortunately we are still not able to include gravity, the last of the four forces, into the SM. There have been attempts to describe gravity through QFT with

[1] Actually U(1) and SU(2) have to be regarded as combined group to be mapped to the electromagnetic-and weak-force in form of the electroweak interaction.

the graviton, a spin-2 boson, as mediator, but there are unsolved problems with the renormalisation of general relativity (GR). Until now GR and quantum mechanics (QM) remain incompatible.

Apart from gravity no being included, the SM has a variety of flaws. One of them is being dependent on many parameters, which have to be measured accurately to perform high-precision physics. In total the Lagrangian of the SM contains 19 parameters. These parameters are represented by ten masses, four CKM-matrix parameters, the QCD-vacuum angle, the Higgs-vacuum expectation value and three gauge coupling constants. Highly accurate values with low errors are crucial for theoretical calculated predictions. One of the major error inputs of every theoretical output are uncertainties in these parameters. In this work we will focus on one of the parameters, namely the strong coupling $\alpha_s$.

The strong coupling is currently measured in six different ways: through $\tau$-decays, QCD-lattice computations, deep inelastic collider results and electroweak precision fits **[PDG2018]**. We have plotted the values of each of the methods in **??**. During this work we will focus on the subfield of $\tau$-decays to measure the value of the strong coupling $\alpha_s(m_\tau)$ at the $\tau$-scale. We will see that in QCD the value of the coupling "constant" depends upon the scale. The $\tau$ is an elementary particle with negative electric charge and a spin of $1/2$. Together with the lighter electron and muon it forms the group of charged Leptons[2]. Even though it is an elementary particle it decays via the weak interaction with a lifetime of $\tau_\tau = 2.9 \times 10^{-13}$ s and has a mass of $1776.86(12)$ MeV**[PDG2018]**. It is furthermore the only lepton massive enough to decay into hadrons, thus of interest for our QCD study. The final states of a decay are limited by conservation laws. In case of a $\tau$-decay they must conserve the electric charge $(-1)$ and invariant mass of the system. Thus, we can see

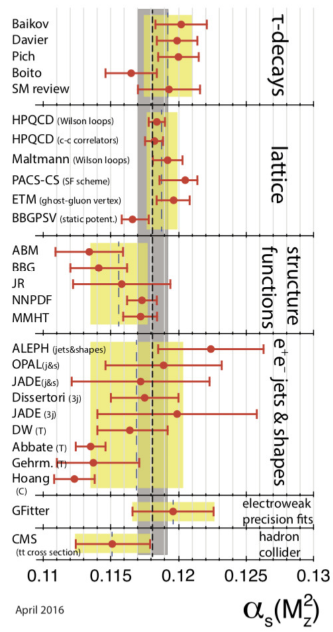


Figure 1.2: The six different subfields and their results for measuring the strong coupling $\alpha_s$ **[PDG2018]**.

[2] Leptons do not interact via the strong force.

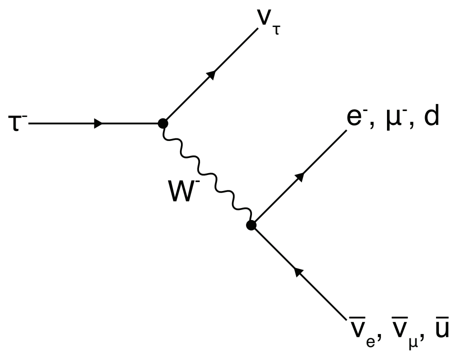


Figure 1.3: Feynman diagram of common decay of a $\tau$-lepton into pairs of lepton-antineutrino or quark-antiquark by the emission of a *W boson*.

| Name | Symbol | Quark content | Rest mass (MeV) |
|---|---|---|---|
| Pion | $\pi^-$ | $\bar{u}d$ | 139.570 61(24) MeV |
| Pion | $\pi^0$ | $(u\bar{u} - d\bar{d})/\sqrt{2}$ | 134.9770(5) MeV |
| Kaon | $K^-$ | $\bar{u}s$ | 493.677(16) MeV |
| Kaon | $K^0$ | $d\bar{s}$ | 497.611(13) MeV |
| Eta | $\eta$ | $(u\bar{u} + d\bar{d} - 2s\bar{s})/\sqrt{6}$ | 547.862(17) MeV |

Table 1.1: List of mesons produced by a $\tau$-decay. Rare final states with branching Ratios smaller than 0.1 have been omitted. The list is taken from [**Davier2006**] with corresponding rest masses taken from [**PDG2018**].

from the corresponding Feynman diagram **??** [3], that
the $\tau$ decays by the emission of a *W*-boson and a tau-neutrino $\nu_\tau$ into pairs of $(e^-, \bar{\nu}_e), (\mu^-, \bar{\nu}_\mu)$ or $(q, \bar{q})$. We are foremost interested into the hadronic decay channels, meaning $\tau$-decays that have quarks in their final states. Quarks have never been measured isolated, but appear always in combination of *mesons* and *baryons*. Due to its mass of $m_\tau \approx 1.8\,\mathrm{GeV}$ the $\tau$-particle decays into light mesons (pions-$\pi$, kaons-K, and eta-$\eta$, see **??**), which can be experimentally detected. The hadronic $\tau$-decay provides one of the most precise ways to determine the strong coupling [**Pich2016**] and is theoretically accessible to high precision within the framework of QCD.

[3] The $\tau$-particle can also decay into strange quarks or charm quarks, but these decays are rather uncommon due to the heavy masses of s and c.

The theory describing strong interactions is QCD. As the name suggest[4] QCD is characterised by the colour charge and is a non-abelian gauge theory with symmetry group SU(3). Consequently every quark has next to its type one of the three colours blue, red or green and the colour force is mediated through eight gluons, which each being bi-coloured[5], interact with quarks and each other. The strength of the strong force is given by the coupling constant $\alpha_s$, which depends on the renormalisation-scale $\mu$. We often chosen the renormalisation-scale in a way that the coupling constant $\alpha_s(q)$ depends on the energy $q^2$. Thus the coupling varies with energy. It increases for low and decreases for high energies[6]. This behaviour has two main implications. The first one states, that for low energies the coupling is too strong for isolated quarks to exist. Until now we have not been able to observe an isolated quark and all experiments can only measure quark compositions. These bound states are called *hadrons* and consist of two or three quarks [7], which are referred to as mesons[8] or baryons [9] respectively. This phenomenon, of quarks sticking together as hadrons is referred to as *confinement*. As the fundamental degrees of freedom of QCD are given by quarks and gluons, but the observed particles are hadrons we need to introduce the assumption of *quark-hadron duality* to match the theory to the experiment. This means that a physical quantity should be similarly describable in the hadronic picture or quark-gluon picture and that both descriptions are equivalent. As we will see in our work quark-hadron duality is violated for low energies. These so-called *duality violations* (DV) have an impact on our strong coupling determinations and can be dealt with either suppression or the inclusion of a model [**Cata2008**]. Throughout this work we will favour and argument for the former approach. The second implication concerns *Perturbative Theory* (PT). The lower the energies we deal with, the higher the value of the strong coupling and the contributions of *Non-Perturbative Theory* (NPT) effects. Currently there are three solutions to deal with *Non-Perturbative* (NP) effects:

- ***Chiral Perturbation Theory*** (CHPT): Introduced by Weinberg [**Weinberg1978**]

[4]Chromo is the Greek word for colour.
[5]Each gluon carries a colour and an anti-colour.
[6]In contrast to the electromagnetic force, where $\alpha(q^2)$ decreases!
[7]There exist also so-called *Exotic hadrons*, which have more than three valence quarks.
[8]Composite of a quark and an anti-quark.
[9]Composite of three quarks or three anti-quarks.

in the late seventies. CHPT is an effective field theory constructed with a Lagrangian symmetric under a chiral-transformation in the limit of massless quarks. It's limitations are based in the chiral symmetry, which is only a good approximation for the light quarks $u$, $d$ and in some cases $s$.

- ***Lattice QCD*** (LQCD): Is the numerical approach to the strong force. Based on the Wilson Loops [**Wilson1974**] we treat QCD on a finite lattice instead of working with continuous fields. LQCD has already many applications but is limited due to its computational expensive calculations.

- ***QCD Sum Rules*** (QCDSR): Was also introduced in the late seventies by Shifman, Vainstein and Zakharov [**Shifman1978**, **Shifman1978a**]. It relates the observed hadronic picture to quark-gluon parameters through a dispersion relation and the use of the *Operator Product Expansion* (OPE), which treats NP effect through the definition of vacuum expectation values, the so-called *QCD condensates*. It is a precise method for extracting the strong coupling $\alpha_s$ at low energies, although limited to the unknown higher order contributions of the OPE.

In this work we focus on the determination of the strong coupling $\alpha_s$ within the framework of QCDSR for $\tau$-decays which has been exploited in the beginning of the nineties by Braaten, Narison and Pich [**Braaten1991**]. Within this setup we can measure $\alpha_s(m_\tau^2)$ at the $m_\tau$ scale. As the strong coupling gets smaller at higher energies, so do the errors. Thus if we obtain the strong coupling at a low scale we will obtain high precision values at the scale of the Z-boson mass $m_Z$, which is the standard scale to compare $\alpha_s$ values.

The QCDSR for the determination of $\alpha_s$, from low energies, contain three major issues.

1. There are two different approaches to treat perturbative and non-perturbative contributions. In particular, there is a significant difference between results obtained using fixed-order (FOPT) or contour improved perturbation theory (CIPT), such that analyses based on CIPT generally arrive at about 7% larger values of $\alpha_s(m_{\tau^2})$ than those based on FOPT [**PDG2018**]. There have been a variety of analyses on the topic been

performed [**Pich2013**, **Caprini2009**, **Jamin2005**] and we will favour the FOPT approach, but generously list our results for the CIPT framework.

2. There are several prescriptions to deal with the NP-contributions of higher order OPE condensates. Typically terms of higher dimension have been neglected, even if they knowingly contribute. In this work we will include every necessary OPE term.

3. Finally there are known DV leading to an ongoing discussion of the importance of contributions from DV. Currently there are two main approaches: Either we neglect them, arguing that they are sufficiently suppressed due to *pinched weights* [**Pich2016**] or model DV with sinusoidal exponentially suppressed function [**Cata2008**, **Boito2011a**, **Boito2014**] introducing extra fitting parameters. We will argue for the former method, implementing pinched weights that sufficiently suppress DV contributions such as having only a negligible effect on our analysis.

In the first chapter of this work we want to summarise the necessary theoretical background for working with the QCDSR. Starting with the basics of QCD we want to motivate the *Renormalisation Group Equation* (RGE), which is responsible for the running of the strong coupling. We then continue with the some aspects of the two-point function and its usage in the dispersion relation, which connects the hadronic picture with the quark-gluon picture. $\cdots$

Chapter 2

# QCD Sum Rules

The theory of QCD was formulated to find one single framework that describes the many hadrons that exist. Unfortunately making use of *perturbative* QCD (PQCD) is limited. QCD predicts a large coupling constant for low energies. As a consequence we can only ever observe hadrons, but our theoretical foundation is ruled by the DOF of quarks and gluons. To extract QCD parameters (the six quark masses and the strong coupling) from hadrons we need to bridge the quark-gluon picture with the hadron picture. To do so we will introduce the framework of QCDSR.

We will start by setting up the foundations of strong interaction with introducing the QCD-Lagrangian. The QCD-Lagrangian is ruled by the abelian gauge group $SU(3)$. The group implies a energy dependence of the coupling and thus limits the applicability of PT for low energies, where the coupling is large. Next we will focus on the two-point function, which plays a major role in the framework of QCDSR. The two-point function is defined as vacuum-expectation values of the time ordered product of two local fields

$$\Pi(q^2) = \int \frac{d^4 q}{(2\pi)^4} e^{iqx} \langle \Omega | T\{\overline{q}(x) q(0)\} | \Omega \rangle. \tag{2.0.1}$$

We can use it to theoretically describe processes, like $\tau$-decays into hadrons, by matching the quantum numbers of the fields, we choose in specifying the two-point function, to the outgoing hadrons. We will see, that the two-point function $\Pi(q^2)$ is related to hadronic states, by poles for $q^2 > 0$. Here NP-effects become important and we need to introduce the OPE, which handles NP parts through QCD-condensates. The condensates form part of the full physical vacuum and would not exist regarding the perturbative vacuum solely. Consequently the condensates are not accessible trough PT methods and have to be fitted from experiment or calculated with the help of NP tools, like LQCD. Finally we will combine a dispersion relation and Cauchy's theorem to finalise the discussion on the QCDSR with developing the *finite energy sum rules* (FESR), which we will apply to extract the strong coupling from tau-decays into hadrons.

## 2.1 Quantum-chromodynamics

Since the formulation of QED in the end of the 40's it had been attempted to describe the strong nuclear force as a QFT, which has been achieved in the 70's as QCD [**GellMann1972**, **Fritzsch1973**, **Gross1973**, **Politzer1973**, **Weinberg1973**]. QCD is a renormalisable QFT constructed to describe the strong interaction. Its fundamental fields are given by dirac spinors of spin-$1/2$, the so-called quarks, with a fractional electric charge of $\pm 1/3$ or $\pm 2/3$. The theory furthermore contains gauge fields of spin 1. These gauge fields are called gluons, do not carry electric charge and are massless. They are the force mediators, which interact with quarks and themselves, because they carry colour charge, in contrast to photons of QED, which interact only with fermions.

The corresponding gauge-group of QCD is the non-abelian group $SU(3)$. Each of the quark flavours $u, d, c, s, t$ and $b$ belongs to the fundamental representation of $SU(3)$ and contains a triplet of fields $\Psi$.

$$\Psi = \begin{pmatrix} \Psi_1 \\ \Psi_2 \\ \Psi_3 \end{pmatrix} \tag{2.1.1}$$

The labels of the triplet are the colours red, green and blue, which play the role of *colour charge*, similar to the electric charge of QED. The gluons belong to the adjoint representation of $SU(3)$, contain an octet of fields and can be expressed using the Gell-Mann matrices $\lambda_a$

$$B_\mu = B_\mu^a \lambda_a \qquad a = 1, 2, \dots 8 \tag{2.1.2}$$

The classical *Lagrange density* of QCD is given by [**Yndurain2006**, **Pascual1984**]:

| Flavour | Mass |
|---|---|
| u | 2.50(17) MeV |
| d | 4.88(20) MeV |
| s | 93.44(68) MeV |
| c | 1.280(13) GeV |
| b | 4.198(12) GeV |
| t | 173.0(40) GeV |

Table 2.1: List of quarks and their masses. The masses of the up, down and strange quark are quoted in the four-flavour theory ($N_f = 2+1+1$ at the scale $\mu = 2\,\text{GeV}$ in the $\overline{MS}$. The charm and bottom quark are also taken in the four-flavour theory and in the $\overline{MS}$ scheme, but at the scales $\mu = m_c$ and $\mu =_b$ correspondingly. All quarks except for the top quark are taken from the *Flavour Lattice Averaging Group* [**FLAG2019**]. The mass of the top quark is not discussed in [**FLAG2019**] and has been taken from [**PDG2018**] from direct observations of top events.

$$\mathcal{L}_{QCD}(x) = -\frac{1}{4}G^a_{\mu\nu}(x)G^{\mu\nu a}(x) + \sum_A \left[\frac{i}{2}\bar{q}^A(x)\gamma^\mu \overleftrightarrow{D}_\mu q^A(x) - m_A\bar{q}^A(x)a^A(x)\right], \tag{2.1.3}$$

with $q^A(x)$ representing the quark fields and $G^a_{\mu\nu}$ being the *gluon field strength tensor* given by:

$$G^a_{\mu\nu}(x) \equiv \partial_\mu B^a_\nu(x) - \partial^a_\nu(x) + gf^{abc}B^b_\mu(x)B^c_\nu(x), \tag{2.1.4}$$

with $f^{abc}$ as *structure constants* of the gauge-group $SU(3)$ and $\overleftrightarrow{D}_\mu$ as covariant derivative acting to the left and to the right. Furthermore we have used $A, B, \ldots = 0, \ldots 5$ as flavour indices, $a, b, \ldots = 0, \ldots, 8$ as colour indices and $\mu, \nu, \ldots = 0, \ldots 3$ as lorentz indices. Explicitly the Lagrangian writes:

$$\begin{aligned}\mathcal{L}_0(x) = &-\frac{1}{4}\left[\partial_\mu G^a_\nu(x) - \partial_\nu G^a_\mu(x)\right]\left[\partial^\mu G^\nu_a(x) - \partial^\nu G^\mu_a(x)\right] \\ &+ \frac{i}{2}\overline{q}^A_\alpha(x)\gamma^\mu\partial_\mu q^A_\alpha(x) - \frac{i}{2}\left[\partial_\mu\overline{q}^A_\alpha(x)\right]\gamma^\mu q^A_\alpha(x) - m_A\overline{q}^A_\alpha(x)q^A_\alpha(x) \\ &+ \frac{g_s}{2}\overline{q}^A_\alpha(x)\lambda^a_{\alpha\beta}\gamma_\mu q^A_\beta(x)G^\mu_a(x) \\ &- \frac{g_s}{2}f_{abc}\left[\partial_\mu G^a_\nu(x) - \partial_\nu G^a_\mu(x)\right]G^\mu_b(x)G^\nu_c(x) \\ &- \frac{g_s^2}{4}f_{abc}f_{ade}G^b_\mu(x)G^c_\nu(x)G^\mu_d(x)G^\nu_e(x)\end{aligned} \tag{2.1.5}$$

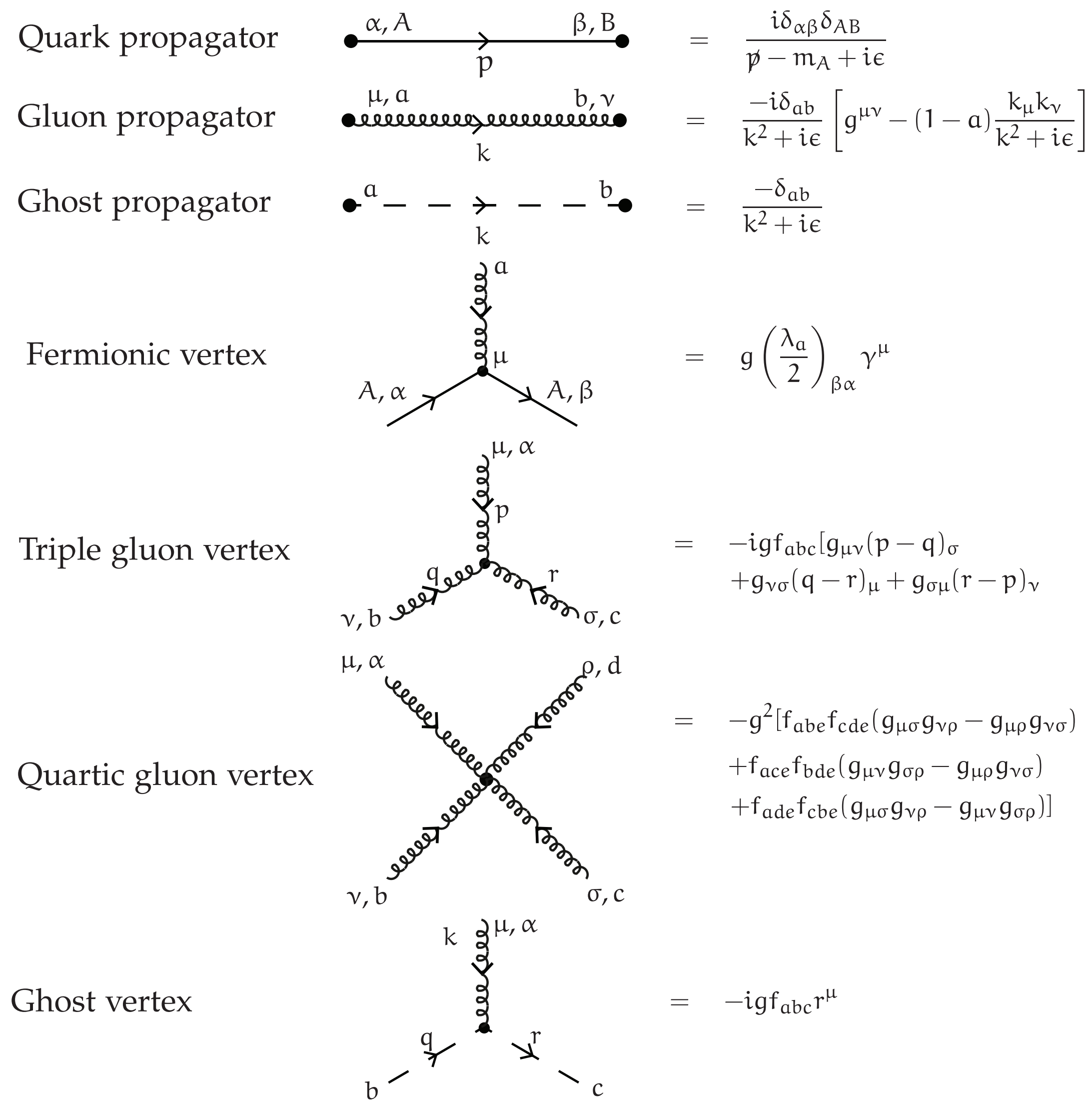


Figure 2.1: QCD Feynman rules.

The first term is the kinetic term for the massless gluons. The next three terms are the kinetic terms for the quark field with different masses for each flavour. The rest of the terms are the interaction terms. The fifth term represents the interaction between quarks and gluons and the last two terms the self-interactions of gluon fields.

The corresponding Feynman rules have been displayed in **??**. The rules are based on PT, but can be enhanced with the QCD condensates, as we will see in the discussion of the OPE in **??**

Having derived the Lagrangian leaves us with its quantisation. The dirac-spinors can be quantised as in QED without any problems. The $\Psi(x)$ quantum field can be written as:

$$\Psi(x) = \int \frac{d^3p}{(2\pi)^3 2E(\vec{p})} \sum_{\lambda} \left[ u(\vec{p},\lambda) a(\vec{p},\lambda) e^{-ipx} + v(\vec{p},\lambda) b^{\dagger}(\vec{p},\lambda) e^{ipx} \right], \qquad (2.1.6)$$

where the integration ranges over the positive sheet of the mass hyperboloid $\Omega_{+}(m) = \{p|p^2 = m^2, p^0 > 0\}$. The four spinors $u(\vec{p},\lambda)$ and $v(\vec{p},\lambda)$ are solutions to the dirac equations in momentum space

$$\begin{aligned} [\not{p} - m] u(\vec{p},\lambda) &= 0 \\ [\not{p} + m] v(\vec{p},\lambda) &= 0, \end{aligned} \qquad (2.1.7)$$

with $\lambda$ representing the helicity state of the spinors.

The quantisation of the gauge fields is more cumbersome. One is forced to introduce supplementary non-physical fields, the so-called Faddeev-Popov ghosts $c^a(x)$ [**Faddeev1967**], to cancel unphysical helicity degrees of freedom of the gluon fields.

The free propagators for the quark, the gluon and the ghost fields are then given by

$$\begin{aligned} iS^{(0)AB}_{\alpha\beta}(x-y) &\equiv q^A_\alpha(x)\bar{q}^B_\beta(y) \equiv \langle 0|T\{q^A_\alpha(x)\bar{q}^B_\beta\}|0\rangle = \delta_{AB}\delta_{\alpha\beta} iS^{(0)}(x-y) \\ &= i\delta_{AB}\delta_{\alpha\beta} \int \frac{d^4p}{(2\pi)^4} \frac{\not{p} + m}{(p^2 - m^2 + i\epsilon)} \\ iD^{(0)\mu\nu}_{ab}(x-y) &\equiv B^\mu_a(x)B^\nu_b(y) \equiv \langle 0|T\{B^\mu_a(x)B^\nu_b(y)\}|0\rangle \equiv \delta_{ab} i \int \frac{d^4k}{(2\pi)^4} D^{(0)\mu\nu}(k) e^{-ik(x-y)} \\ &= i\delta_{ab} \int \frac{d^4k}{(2\pi)^4} \frac{1}{k^2 + i\epsilon} \left[ -g_{\mu\nu} + (1-a)\frac{k_\mu k_\nu}{k^2 + i\epsilon} \right] e^{-ik(x-y)} \\ i\widetilde{D}^{(0)}_{ab}(x-y) &\equiv \phi_a(x)\bar{\phi}_b(y) \equiv \langle 0|T\{\phi_a(x)\bar{\phi}_b(y)\}|0\rangle = \frac{i}{(2\pi)^4}\delta_{ab} \int d^4q \frac{-1}{q^2 + i\epsilon} e^{-q(x-y)} \\ &\equiv \frac{i}{(2\pi)^4}\delta_{ab} \int d^4q\, \widetilde{D}^{(0)}(q) e^{-iq(x-y)}, \end{aligned} \qquad (2.1.8)$$

The previously introduced Feynman rules and propagators all make use of the perturbative vacuum $|0\rangle$ and are thus counted as tools of PT. Consequently they need a small coupling to approximate excitations of full QCD vacuum. We will see in the following section, that the strong coupling runs with energy and unfortunately is large for small energy scales.

### 2.1.1 Renormalisation Group

Computing observables with the QCD Lagrangian (**??**) lead to divergencies, which have to be *renormalised*. To render these divergent quantities finite we have to introducing a suitable parameter such that the "original divergent theory" corresponds to a certain value of that parameter. These procedure is referred to as *regularisation* and there are various approaches:

- **Cut-off regularisation:** In cut-off regularisation we limit the divergent momentum integrals by a cut-off $|\vec{p}| < \Lambda$. Here $\Lambda$ has the dimension of mass. The cut-off regularisation breaks translational invariance, which can be guarded by making use of other regularisation methods.

- ***P-V* (Pauli-Villars) regularisation: [Pauli1949]** In P-V regularisation the propagator is forced to decrease faster than the divergence to appear. It replaces the nominator by

$$(\vec{p}^2 + m^2)^{-1} \to (\vec{p}^2 + m^2)^{-1} - (\vec{p}^2 + M^2)^{-1}, \tag{2.1.9}$$

  where $M$ has the dimension acts similar as the previously presented cut-off, but conserves translational invariance.

- **Dimensional regularisation: [Bollini1972, tHooft1972, tHooft1973]** Dimensional regularisation has been introduced in the beginning of the seventies to regularise non-abelian gauge theories (like QCD), where $\Lambda$- and P-V-regularisation failed. In dimensional regularisation we expand the four space-time dimensions to arbitrary $D$-dimensions. To compensate for the additional dimensions we introduce an additional scale $\mu^{D-4}$. A typical Feynman-integral then has the following appearance:

$$\int \frac{d^4 p}{(2\pi)^4} \frac{1}{\vec{p}^2 + m^2} \to \mu^{2\epsilon} \int \frac{d^D p}{(2\pi)^D} \frac{1}{\vec{p}^2 + m^2}, \tag{2.1.10}$$

  Dimensional regularisation preserves all symmetries, it allows an easy identification of divergences and naturally leads to the *minimal subtraction scheme* (MS) **[tHooft1973, Weinberg1973a]**.

In all of the three regularisation schemes we introduced an arbitrary parameter to regularise the divergence. This parameter causes scale dependence of the strong coupling and the quark masses. As we are mainly concerned with the non-abelian gauge theory QCD we will focus on dimensional regularisation, which introduced the parameter $\mu$. Measurable observables (*Physical quantities*) cannot depend on the renormalisation scale $\mu$. Therefore the derivative by $\mu$ of a general physical quantity has to yield zero. A physical quantity $R(q, a_s, m)$, that depends on the external momentum $q$, the renormalised coupling $a_s \equiv \alpha_s/\pi$ and the renormalised quark mass $m$ can then be expressed as

$$\mu \frac{d}{d\mu} R(q, a_s, m) = \left[\mu \tfrac{\partial}{\partial \mu} + \mu \tfrac{d a_s}{d\mu} \tfrac{\partial}{\partial m} + \mu \tfrac{dm}{d\mu} \tfrac{\partial}{\partial m}\right] R(q, a_s, m) = 0. \tag{2.1.11}$$

**??** is referred to as a *renormalisation group equation* (RGE) and is the basis for defining the two *renormalisation group functions*:

$$\beta(a_s) \equiv -\mu \tfrac{d a_s}{d\mu} = \beta_1 a_s^2 + \beta_2 a_s^3 + \dots \qquad \beta-\text{function} \tag{2.1.12}$$

$$\gamma(a_s) \equiv -\frac{\mu}{m} \tfrac{dm}{d\mu} = \gamma_1 a_s + \gamma_2 a_s^2 + \dots \qquad \text{anomalous mass dimension.} \tag{2.1.13}$$

The $\beta$-function dictates the running of the strong coupling, whereas the anomalous mass dimension describes the running of the quark masses. We have a special interest in the running of the strong coupling, but will also shortly sum up the running of the quark masses.

### Running gauge coupling

Regarding the $\beta$-function we notice, that $a_s(\mu)$ is not a constant, but that it *runs* by varying its scale $\mu$. To better understand the running of the strong coupling we integrate the $\beta$-function

$$\int_{a_s(\mu_1)}^{a_s(\mu_2)} \frac{d a_s}{\beta(a_s)} = -\int_{\mu_1}^{\mu_2} \frac{d\mu}{\mu} = \log \frac{\mu_1}{\mu_2}. \tag{2.1.14}$$

To analytically evaluate the above integral we can approximate the $\beta$-function to first order, with the known coefficient

$$\beta_1 = \frac{1}{6}(11 N_c - 2 N_f), \tag{2.1.15}$$

yielding

$$a_s(\mu_2) = \frac{a_s(\mu_1)}{\left(1 - a_s(\mu_1)\beta_1 \log \frac{\mu_1}{\mu_2}\right)}. \tag{2.1.16}$$

**??** has some important implications for the strong coupling:

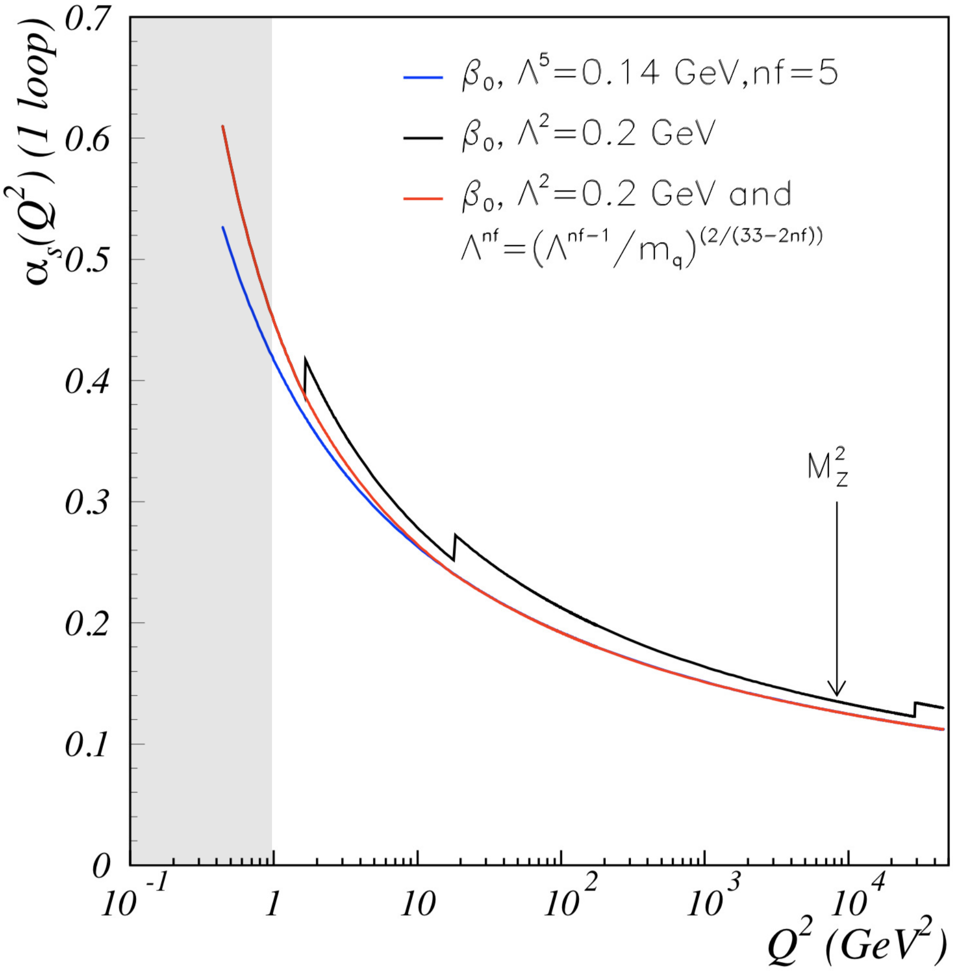


Figure 2.2: Running of the strong coupling $\alpha_s(Q^2)$ at first order. The blue line represents the uncorrected coupling constant, with an $\Lambda^{nf=5}$ chosen to match an experimental value of the coupling at $Q^2 = M_Z^2$. The quark-thresholds are shown by the black line and the corrected running is given by the red line. We additionally marked the breakdown of pt with a grey background for $Q^2 < 1$. The image is taken from an recent review of the strong coupling **[Deur2016]**.

- The coupling at a scale $\mu_2$ depends on $a_s(\mu_1)$. Thus we have to take care of the scale $\mu$, while comparing different values of $\alpha_s$. In the literature (e.g. **[pdg2016]**) $\alpha_s$ is commonly compared at the Z-boson scale of around 91 GeV. As we are extracting the strong coupling at the mass of the tau lepton, around 1.776 GeV we need to run the strong coupling up to the desired scale. While running the coupling, we have to take care of the quark-thresholds. Each quark gets active at a certain energy scale, which leads to a running of $\alpha_s$ as shown in **??**. Typically one runs the coupling with the aid of software packages like *RunDec* [**Chetyrkin2000**, **Herren2017**], which has also been ported to support C (*CRunDec*, [**Schmidt2012**]) and Python [**Straub2016**].

- As we have three colours ($N_c = 3$ and six flavours ($N_f = 6$ the first $\beta_1$ coefficient **??** is positive. Thus for $\mu_2 < \mu_1$ $a_s(\mu_2)$ increases logarithmically and at a scale of $\mu_2 = 1$ GeV reaches a value of

$$\alpha_s(1\,\mathrm{GeV}) \approx 0.5, \tag{2.1.17}$$

  which questions the applicability of PT for energies lower than 1 GeV (as seen from the grey zone in **??**).

- A large coupling for small scales implies confinement. We are not able to separate quarks in a meson or baryon. No quark has been detected as single particle yet. This is qualitatively explained with the gluon field carrying colour charge. These gluons form so-called *flux-tubes* between quarks, which cause a constant strong force between particles regardless of their separation. Consequently the energy needed to separate quarks is proportional to the distance between them and at some point there is enough energy to favour the creation of a new quark pair. Thus before separating two quarks we create a quark-antiquark pair. As a result we will probably never be able to observe an isolated quark. This phenomenon is referred to as colour confinement or simply confinement.

- With the first $beta_1$ coefficient being positive we notice that for increasing scales ($\mu_2 > \mu_1$) the coupling decreases logarithmically. This leads to asymptotic freedom, which states, that for high energies (small distances), the strong coupling becomes diminishing small and quarks and gluons do not interact. Thus in isolated baryons and mesons the quarks are separated by small distances, move freely and do not interact.

From the RGE we have seen, that not only the coupling but also the masses carry an energy dependencies.

### Running quark mass

The mass dependence on energy is governed by the *anomalous mass dimension* $\gamma(a_s)$. Its properties of the running quark mass can be derived similar to the gauge coupling. Starting from integrating the *anomalous mass dimension* **??**

$$\log \frac{m(\mu_2)}{m(\mu_1)} = \int_{a_s(\mu_1)}^{a_s(\mu_2)} da_s \frac{\gamma(a_s)}{\beta(a_s)} \tag{2.1.18}$$

we can approximate the *anomalous mass dimension* to first order and solve the integral analytically **[Schwab2002]**

$$m(\mu_2) = m(\mu_1) \left( \frac{a(\mu_2)}{a(\mu_1)} \right)^{\frac{\gamma_1}{\beta_1}} \left(1 + \mathcal{O}(\beta_2, \gamma_2)\right). \tag{2.1.19}$$

As $\beta_1$ and $\gamma_1$ (see **??**) are positive the quark mass decreases with increasing $\mu$. The general relation between different scales is given by

$$m(\mu_2) = m(\mu_1) \exp\left( \int_{a_s(\mu_1)}^{a_s(\mu_2)} da_s \frac{\gamma(a_s)}{\beta(a_s)} \right) \tag{2.1.20}$$

and can be solved numerically to run the quark mass to the needed scale $\mu_2$. Both, the $\beta$-function and the anomalous mass dimension are currently known up to the $5^{\text{th}}$ order and listed in the appendix **??**.

QCD in general has a precision problem caused by uncertainties and largeness of the strong coupling constant $\alpha_s$. The fine-structure constant (the coupling QED) is known to eleven digits, whereas the strong coupling is only known to about four. Furthermore for low energies the strong coupling constant is much larger than the fine-structure constant. E.g. at the Z-mass, the standard mass to compare the strong coupling, we have an $\alpha_s$ of 0.11, whereas the fine structure constant would be around 0.007. Consequently to use PT we have to calculate our results to much higher orders, including tens of thousands of Feynman diagrams, in QCD to achieve a precision equal to QED. For even lower energies, around 1 GeV, the strong coupling reaches a critical value of around 0.5 leading to a break down of PT.

In this work we try to achieve a higher precision in the value of $\alpha_s$. The framework we use to measure the strong coupling constant are the QCDSR. A central object needed to describe hadronic states with the help of QCD is the *two-point function* for which we will devote the following section.

## 2.2 Two-Point function

In analogy to the Green function for elemental fields we can define a propagator for composite currents, referred to as *two-point function*

$$\Pi(x) = \langle\Omega|T\{J(x)J(y)\}|\Omega\rangle, \tag{2.2.1}$$

where $T\{\cdots\}$ is the time-ordered product and $|\Omega\rangle$ is the ground state/ vacuum of the interacting theory. Note that the fields are in general given in the Heisenberg picture, which implies translational invariance.

$$\begin{aligned} \langle\Omega|\phi(x)\phi(y)|\Omega\rangle &= \langle\Omega|\phi(x)e^{i\hat{P}y}e^{-i\hat{P}y}\phi(y)e^{i\hat{P}y}e^{-i\hat{P}y}|\Omega\rangle \\ &= \langle\Omega|\phi(x-y)\phi(0)|\Omega\rangle, \end{aligned} \tag{2.2.2}$$

where we made use of the translation operator $\hat{T}(x) = e^{-i\hat{P}x}$.

In this work we are solely concerned about the *two-point function*, especially in the vacuum expectation value of the Fourier transform of two time-ordered QCD quark Noether currents

$$\Pi_{\mu\nu}(p^2) \equiv \int \frac{d^4x}{(2\pi)^4} e^{ipx}\langle\Omega|T\left\{J_\mu(x)J_\nu(0)\right\}|\Omega\rangle, \tag{2.2.3}$$

where the Noether current is given by

$$J_\mu(x) = \overline{q}\,(x)\Gamma q(x). \tag{2.2.4}$$

Here, $\Gamma$ can be any of the following dirac matrices $\Gamma \in \{1, i\gamma_5, \gamma_\mu, \gamma_\mu\gamma_5\}$, specifying the quantum number of the current (S: *scalar*, P: *pseudo-Scalar*, V: *vectorial*, A: *axial-vectorial*, respectively). By choosing the right quantum numbers we can theoretically represent the processes we want to study, which will be important when we want to theoretically describe the hadrons produced in $\tau$-decays.

From a Feynman diagram point of view we can illustrate the two-point function as quark-antiquark pair, which is produced by an external source, e.g. the virtual $W$-boson of $\tau\bar{\tau}$-annihilation as seen in **??**. Here the quarks are propagating at *short-distances*, which implies that we can make use of PT, thus avoiding *long-distance* (NPT-) effects, that would appear if the initial and final states where given by hadrons [**Colangelo2000**]. It is interesting to note, that the same process with the help of the *optical theorem* can be used to derive the total decay width of hadronic tau decays.

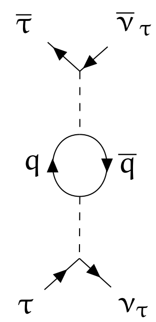


Figure 2.3: $\tau\bar{\tau}$-annihilation with a quark-antiquark pair.

### 2.2.1 Short-Distances vs. Long-Distances

If we want to calculate the two-point function in QCD we have to differentiate short-and long-distances or large or small momenta. In general when we talk about small distances we refer to large momenta. Large momenta implies a small strong coupling constant. Consequently we can use PT for short-distances without problems. On the contrary long distances involve small momenta, which implies a large coupling constant. Thus for long distances the NP effects become important and have to be dealt with. To apply PT to the case of the $\tau\bar{\tau}$ annihilation we need the quark-antiquark pair of **??** to be highly virtual [1]. To roughly separate long-distances from short-distances using a length scale we can say that the length scale should be smaller than the radius of a hadron.

### 2.2.2 Relating Two-Point Function and Hadrons

The two-point function can be interpreted physically as the amplitude of propagating single- or multi-particle states and their excitations. The possible

[1] Which is the same of saying, that the quark-antiquark pair needs a high external momentum $q$.

| Symbol | Quark content | Isospin | J | Current |
|---|---|---|---|---|
| $\pi^+$ | $u\overline{d}$ | 1 | 0 | $: u\gamma_\mu\gamma_5\overline{d} :$ |
| $\pi^0$ | $\frac{u\overline{u}-d\overline{d}}{2}$ | 1 | 0 | $: \overline{u}\gamma_\mu\gamma_5 u + \overline{d}\gamma_\mu\gamma_5 d :$ |
| $\eta$ | $\frac{u\overline{u}+d\overline{d}-2s\overline{s}}{\sqrt{6}}$ | 0 | 0 | $: \overline{u}\gamma_\mu\gamma_5 u + \overline{d}\gamma_\mu\gamma_5 d - 2\overline{s}\gamma_\mu\gamma_5 s :$ |
| $\eta\prime$ | $\frac{u\overline{u}+d\overline{d}+s\overline{s}}{\sqrt{3}}$ | 0 | 0 | $: \overline{u}\gamma_\mu\gamma_5 u + \overline{d}\gamma_\mu\gamma_5 d + \overline{s}\gamma_\mu\gamma_5 s :$ |
| $\rho^0$ | $\frac{u\overline{u}-d\overline{d}}{\sqrt{2}}$ | 1 | 1 | $: \overline{u}\gamma_\mu u - \overline{d}\gamma_\mu d :$ |
| $\omega$ | $\frac{u\overline{u}+d\overline{d}}{\sqrt{2}}$ | 0 | 1 | $: \overline{u}\gamma_\mu u + \overline{d}\gamma_\mu d :$ |
| $\phi$ | $s\overline{s}$ | 0 | 1 | $: \overline{s}\gamma_\mu\gamma_5 s :$ |
| $K^+$ | $u\overline{s}$ | $\frac{1}{2}$ | 0 | $: u\gamma_\mu\gamma_5\overline{s} :$ |
| $K^0$ | $d\overline{s}$ | $\frac{1}{2}$ | 0 | $: d\gamma_\mu\gamma_5\overline{s} :$ |

Table 2.2: Ground-state vector and pseudoscalar mesons for the light-quarks $u, d$ and $s$ with their corresponding currents in the two-point function. Note that we use $\gamma_\mu$ for vector and $\gamma_\mu\gamma_5$ for the pseudoscalar mesons.

states, in our case, the hadrons we describe through the correlator are fixed by the quantum numbers of the current we define for the vacuum expectation value. For example the neutral $\rho$-meson is a spin-1 vector meson with a quark content of $(u\overline{u} - d\overline{d})/\sqrt{2}$. Consequently by choosing a current

$$J_\mu(x) = \frac{1}{2}(\overline{u}(x)\gamma_\mu u(x) - \overline{d}(x)\gamma_\mu d(x)) \tag{2.2.5}$$

the two-point function contains the same quantum numbers as the $\rho$-meson and is said to materialise to it. A list of some ground-state mesons for combinations of the light quarks $u, d$ and $s$ is given in **??**.

The correlator is materialising into a spectrum of hadrons. Thus if we insert a complete set of states of hadrons we can make use of the unitary relation

$$\langle\Omega|J_\mu(x)_\nu(0)|\Omega\rangle = \sum_X \langle\Omega|J_\mu(x)|X\rangle\langle X|J_\nu(0)|\Omega\rangle. \tag{2.2.6}$$

to represent the two-point correlator via a spectral function $\rho(t)$

$$\Pi(p^2) = \int_0^\infty ds \frac{\rho(s)}{s - p^2 - i\epsilon}. \tag{2.2.7}$$

The above relation is referred to as *Källén-Lehmann spectral representation* [**Kallen1952**, **Lehmann1954**] or *dispersion relation*. It relates the two-point function to the spectral function $\rho$, which can be represented as sum over all possible hadronic states

$$\rho(s) = (2\pi)^3 \sum\!\!\!\!\!\!\!\int_X \left|\langle \Omega | J_\mu(0) | X \rangle\right|^2 \delta^4(s - p_X). \tag{2.2.8}$$

Note that the analytic properties of the two-point are in one-to-one correspondence with the newly introduced spectral function and thus determined by the possible hadrons states, which only form on the positive real axis. A full derivation of the *Källén-Lehmann spectral representation* can be found in the appendix **??**. The spectral function is interesting to us for two reasons. First it is experimentally measurable and second it carries a problematic "branch cut", which we want to discuss now.

### 2.2.3 Analytic Structure of the Two-Point Function

The general two-point function $\rho(s)$ has some interesting analytic properties. It has poles for single-particle states and a continuous branch cut for multi-particle states. The single and multi-particle states, for a general correlator, can be mathematically separated by

$$\rho(s) = Z\delta(s - m^2) + \theta(s - s_0)\sigma(s), \tag{2.2.9}$$

where the second term is the contribution from multi-particle states. $\sigma(s)$ is zero till we reach the threshold, where we have sufficient energy to form multi-particle states. The analytic structure is depicted by **??** and we can see that the spectral function has $\delta$-spikes for single-particle states and a continuous contribution for $s \geqslant 4m$ resulting from multi-particle states. These lead to poles and a continuous branch cut of the two-point function.

### 2.2.4 Decompositions

Apart the spectral decomposition we can also Lorentz decompose the two-point function or write it in terms of *vector* (V), *axial-vector* (A), *scalar* (S) and *pseudo-scalar* (P) contributions.

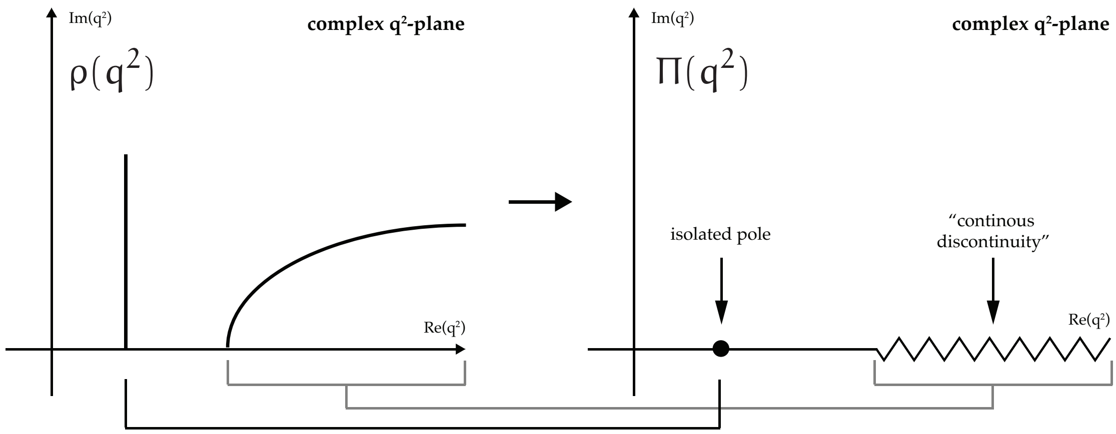


Figure 2.4: Analytic structure in the complex $q^2$-plane of the Fourier transform of the two-point function. The hadronic final states are responsible for poles appearing on the real-axis. The one-particle states contribute as isolated pole and the multi-particle states contribute as bound-states poles or a continues "discontinuity cut" [**Peskin1995**, **Zwicky2016**].

### Lorentz decomposition

Due to the Lorentz invariance of the two-point function, and by assuming the conservation of the Noether current, we can apply the Ward identity to decompose the correlator $\Pi_{\mu\nu}$ into its scalar contribution $\Pi$.

There exist only two possible terms that can guard the structure of the second order tensor: $q_\mu q_\nu$ and $q^2 g_{\mu\nu}$. The sum of both multiplied with two arbitrary functions $A(q^2)$ and $B(q^2)$ yields

$$\Pi_{\mu\nu}(q^2) = q_\mu q_\nu A(q^2) + q^2 g_{\mu\nu} B(q^2). \tag{2.2.10}$$

By assuming that we deal with equal quark flavours and that the vector current is conserved, i.e. $\partial^\mu j_\mu() = 0$, we can make use of the *Ward-identity*

$$q^\mu \Pi_{\mu\nu} = 0 \tag{2.2.11}$$

to demonstrate, that the two arbitrary functions are related

$$\begin{aligned} q^\mu q^\nu \Pi_{\mu\nu} &= q^4 A(q^2) + q^4 B(q^2) = 0 \\ &\implies A(q^2) = -B(q^2). \end{aligned} \tag{2.2.12}$$

Thus redefining $A(q^2) \equiv \Pi(q^2)$ we expressed the correlator as a scalar function of spin 1

$$\Pi_{\mu\nu}(q^2) = (q_\mu q_\nu - q^2 g_{\mu\nu})\Pi^{(1)}(q^2). \tag{2.2.13}$$

In case of a current of different quark flavours, the current will not be conserved and we cannot apply the Ward identity. Consequently the standard lorentz decomposition into transversal and longitudinal components reads

$$\Pi^{\mu\nu}(q^2) = (q^\mu q^\nu - g^{\mu\nu} q^2)\Pi^{(1)}(q^2) + q^\mu q^\nu \Pi^{(0)}(q^2). \tag{2.2.14}$$

### Transversal and Longitudinal Relations

By comparing the standard lorentz decomposition (**??**) with the decomposition into V/A and S/P parts we can identify the longitudinal components of the correlator as being purely scalar. The latter decomposition can be written as **[Broadhurst1981, Jamin1992]**

$$\begin{aligned} q^2\Pi^{\mu\nu}(q^2) = (q^\mu q^\nu - q^2 g^{\mu\nu})\Pi^{V,A}(q^2) + g^{\mu\nu}(m_i \mp m_j)\Pi^{S,P}(q^2) \\ + g^{\mu\nu}(m_i \mp m_j)\left[\langle\Omega|\overline{q}_i q_i|\Omega\rangle \mp \langle\Omega|\overline{q}_j q_j|\Omega\rangle\right], \end{aligned} \tag{2.2.15}$$

where the third term is a correction arising due to the physical vacuum $|\Omega\rangle$. By multiplying **??** by two four-momenta and making use of the Ward identity **??** we can write

$$q_\mu q_\nu \Pi^{\mu\nu}(q^2) = (m_i \mp m_j)^2 \Pi^{S,P}(q^2) + (m_i \mp m_j)[\langle\overline{q}_i q_i\rangle \mp \langle\overline{q}_j q_j\rangle], \tag{2.2.16}$$

which then can be related to the longitudinal component of **??** by comparison with

$$q_\mu q_\nu \Pi^{\mu\nu}(q^2) = q^4 \Pi^{(0)}(q^2) = s^2 \Pi^{(0)}(s) \quad \text{with} \quad s \equiv q^2, \tag{2.2.17}$$

leading to

$$s^2\Pi^{(0)}(s) = (m_i \mp m_j)^2 \Pi^{(S,P)}(s) + (m_i \mp m_j)[\langle\overline{q}_i q_i\rangle \mp \langle\overline{q}_j q_j\rangle]. \tag{2.2.18}$$

Note that all appearing mass terms are related to the longitudinal component.

As the tau decays, with the limiting factor of the tau mass, can only decay into light quarks we will often neglect the quark masses and work in the so called *chiral limit* ($m_q \to 0$), in which the longitudinal component is going to vanish.

By defining a combination of the transversal and longitudinal correlator

$$\Pi^{(1+0)}(s) \equiv \Pi^{(1)}(s) + \Pi^{(0)}(s) \tag{2.2.19}$$

we can additionally relate the transversal and vectorial components via

$$\Pi^{\mu\nu}(s) = \underbrace{(q^\mu q^\nu - g^{\mu\nu} q^2)\Pi^{(1)}(s) + (q^\mu q^\nu - g^{\mu\nu} q^2)\Pi^{(1)}(s)}_{=(q^\mu q^\nu - g^{\mu\nu} q^2)\Pi^{(1+0)}(s)} + \frac{g^{\mu\nu} s^2}{q^2}\Pi^{(0)}(s), \quad (2.2.20)$$

such that

$$\Pi^{(V,A)}(s) = \Pi^{(1)}(s) + \Pi^{(0)}(s) = \Pi^{(1+0)}(s), \quad (2.2.21)$$

where the vector/ axial-vector component of the correlator is now related to the newly defined transversal and longitudinal combination of the correlator.

Having dealt exclusively with the perturbative part of the theory, we have to discuss NP contributions. These arise due to non negligible long-distance effects. Thus to complete the needed ingredients for *Sum Rules* we need a final ingredient the *Operator Product Expansion* (OPE), which treats the non-perturbative contributions of our theory.

## 2.3 Operator Product Expansion

The OPE was introduced by Wilson in 1969 **[Wilson1969]** as an alternative to the in this time commonly used current-algebra. The expansion states that products of operators at different space-time points can be rewritten into a sum of composite local operators and their corresponding coefficients:

$$\lim_{x\to y} A(x)B(y) = \sum_n C_n(x-y)\mathcal{O}_n(x), \quad (2.3.1)$$

where $C_n(x-y)$ are the so-called *Wilson coefficients* and $A, B$ and $\mathcal{O}_n$ are operators.

The OPE lets us separate short distances from long distances. In pure PT we can only amount for short distances, which are equal to high energies, where the strong coupling $\alpha_s$ is small. The OPE on the other hand accounts for long-distance effects with higher dimensional operators. Applying the OPE to the two-point function we get a sum over the vacuum expectation values

$$\Pi_{\text{OPE}}(q^2) = -\frac{1}{3q^2}\sum_n \langle\Omega|\mathcal{O}_n(0)|\Omega\rangle \int d^4x\, e^{iqx} C_n(x) \quad (2.3.2)$$

The form of the composite operators are dictated by gauge- and Lorentz symmetry. For the two-point function in **??** we only have to consider operators $\mathcal{O}_n$ of dimension

$$d\left(\mathcal{O}_n\right) \leqslant (D-4) + 2N \tag{2.3.3}$$

The scalar operators up to dimension six are then given by **[Pascual1984]**

$$\begin{aligned}
\text{Dimension 0:}\quad & \mathbb{1} \\
\text{Dimension 4:}\quad & :m_i \overline{q}\, q: \\
& :G_a^{\mu\nu}(x) G^a_{\mu\nu}(x): \\
\text{Dimension 6:}\quad & :\overline{q}\,\Gamma q \overline{q}\,\Gamma q: \\
& :\overline{q}\,\Gamma \tfrac{\lambda^a}{2} q_\beta(x) \overline{q}\,\Gamma \tfrac{\lambda^a}{2} q: \\
& :m_i \overline{q}\, \tfrac{\lambda^a}{2} \sigma_{\mu\nu} q G_a^{\mu\nu}: \\
& :f_{abc} G_a^{\mu\nu} G_b^{\nu\delta} G_c^{\delta\mu}:,
\end{aligned} \tag{2.3.4}$$

where $\Gamma$ stands for one of possible dirac matrices (as seen **??**). Note, that the $D = 2$ operator violates gauge symmetry and is consequently excluded from our list. Within PT only the unit operator would exist, as the higher dimensional operators would appear as normal ordered products of fields and vanish by being sandwiched into the perturbative vacuum. On the contrary, in NP QCD they appear as *condensates*. Condensates are the vacuum expectation values of non-vanishing normal ordered fields by applying the full QCD vacuum, which contribute to all strong processes. For example the condensates of dimension four are the quark-condensate $m_i\langle\overline{q}\, q\rangle$ and the gluon-condensate $\langle G G\rangle$.

As long as working with dimensionless functions (e.g. the correlator $\Pi$ in **??**), the *right-hand side* (RHS). of **??** has to be dimensionless. As a result the Wilson coefficients have to cancel the dimension of the operator with their inverse mass dimension. To account for the dimensions we can make the inverse momenta explicit

$$\Pi^{\mathrm{OPE}}_{V/A}(s) = \sum_{D=0,2,4\ldots} \frac{C^{(D)} \langle \Omega | \mathcal{O}^{(D)}(x) | \Omega \rangle}{(-q^2)^{D/2}}, \tag{2.3.5}$$

where we used $c^{(D)} = C^{(D)}/(-s)^{D/2}$ with $D$ being the dimension. Thus the OPE should converge with increasing dimension for sufficiently large momenta $s$.

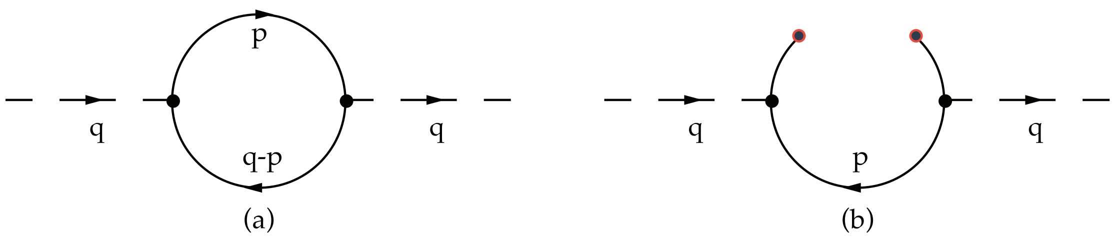


Figure 2.5: Feynman diagrams of the perturbative (a) and the quark-condensate (b) contribution. The upper part of the right diagram is not Wick contracted and responsible for the condensate.

### 2.3.1 A practical example

Let's show how the OPE contributions are calculated with a standard example [**Shifman1978**, **Pascual1984**]. We will compute the perturbative and quark condensate Wilson coefficients for the $\rho$ meson. To do so we have to evaluate Feynman diagrams using standard PT.

The $\rho$ meson is a vector meson of isospin one composed of $u$ and $d$ quarks. As a result (see. **??**) we can match its quantum numbers with the current

$$J^{\mu}(x) = \frac{1}{2}\Big( : [\overline{u}\,\gamma^{\mu}u](x) - [\overline{d}\,\gamma^{\mu}d](x) : \Big)\,. \tag{2.3.6}$$

Pictorial the dimension zero contribution is given by the quark-antiquark loop Feynman diagram **??**. The higher dimension contributions are given by the same Feynman diagram, but with non contracted fields. These non contracted fields contain the condensates. Thus not contracting the quark-antiquark field (see. **??** b) will give us access to the Wilson coefficient of the dimension four quark condensate $m_i\langle\overline{q}\,q\rangle$.

The perturbative part (the Wilson coefficient of dimension zero) can than be taken from the mathematical expression for the scalar correlator

$$\begin{aligned}\Pi(q^2) = -\frac{i}{4q^2(D-1)}\int d^D\, x e^{iqx}\langle\Omega|T\{: \overline{u}\,(x)\gamma^{\mu}u(x) - \overline{d}\,(x)\gamma^{\mu}d(x) :\\ \times : \overline{u}\,(0\gamma_{\mu}u(0) - \overline{d}\,(0)\gamma_{\mu}d(0) :\}\rangle.\end{aligned} \tag{2.3.7}$$

To extract the dimension zero Wilson coefficient we apply Wick's theorem to contract all of the fields, which represents the lowest order of the perturbative contribution. The calculation is only using standard PT and we will restrict ourselves in displaying the result and omitting the calculation[2].

$$\begin{aligned}\Pi(q^2) &= \frac{i}{4q^2(D-1)}(\gamma^\mu)_{ij}(\gamma_\mu)_{kl}\int d^D x e^{iqx} \\ &\times \quad \left[u_{j\alpha}(x)\overline{u}_{k\beta}(0)\cdot u_{l\beta}(0)\overline{u}_{i\alpha}(x) + (u\to d)\right] \\ &= \frac{3}{8\pi^2}\left[\frac{5}{3} - \log\left(-\frac{q^2}{\nu^2}\right)\right].\end{aligned} \tag{2.3.8}$$

To calculate the higher dimensional contributions of the OPE we use the same techniques as before. We apply Wick's theorem, but in this case, due to the NP vacuum, we have non-vanishing vacuum expectation value of normal ordered products of fields. Thus some of the fields are left uncontracted, as can be graphically seen in **??**. For leaving the quark field uncontracted in **??** we get

$$\begin{aligned}\Pi(q^2) = \frac{i}{4q^2(D-1)}(\gamma^\mu)_{ij}(\gamma_\mu)_{kl}\int d^D x e^{iqx} \Big[ \\ + u_{j\alpha}(x)\overline{u}_{k\beta}(0)\cdot\langle\Omega| : \overline{u}_{i\alpha}(x)u_{l\beta}(0) : |\Omega\rangle \\ + u_{l\beta}(0)\overline{u}_{i\alpha}(x)\cdot\langle\Omega| : \overline{u}_{k\beta}(0)u_{j\alpha}(x) : |\Omega\rangle + (u\to d)\Big],\end{aligned} \tag{2.3.9}$$

where $(u \to d)$ is representing the previous expressions with $u$ and $d$ interchanged. Here we can observe the condensates as non-vanishing vacuum values of normal ordered product of fields:

$$\langle\Omega_{QCD}| : \overline{q}(x)q(0) : |\Omega_{QCD}\rangle \neq 0. \tag{2.3.10}$$

We emphasised the QCD vacuum $\Omega_{QCD}$, which is responsible for vacuum expectation values different than zero. E.g. for a vacuum of QED this contributions would vanish by definition. Pictorial the condensates take form of unconnected propagators, sometimes marked with an $\times$, as seen in **??**.

To make the non-contracted fields local, we can expanded them in $x$

$$\begin{aligned}\langle\Omega| : \overline{q}(x)q(0) : |\Omega\rangle &= \langle\Omega| : \overline{q}(0)q(0) : |\Omega\rangle \\ &\quad + \langle\Omega| : \left[\partial_\mu\overline{q}(0)\right] q(0) : |\Omega\rangle x^\mu + \dots,\end{aligned} \tag{2.3.11}$$

where terms with derivatives lead to higher dimensional operators, which can be seen by applying the equation of motions. We then can focus on the first term and introduce a standard notation for the localised condensate

$$\langle\overline{q}\,q\rangle \equiv \langle\Omega| : \overline{q}(0)q(0) : |\Omega\rangle. \tag{2.3.12}$$

[2]The interested reader can follow **[Pascual1984]** for a detailed calculation.

Finally, the contribution to the ρ scalar correlator is then given by the following expression

$$\Pi_{(\rho)}(q^2) = \frac{1}{2}\frac{1}{\left(-q^2\right)^2}\left[m_u\langle\overline{u}\,u\rangle + m_d\langle\overline{d}\,d\rangle\right]. \qquad (2.3.13)$$

Here we can clearly see that for dimension four we get a factor of $1/(-q^2)^2$, which is responsible for the suppression of the series. The condensates $\langle\overline{u}\,u\rangle$ and $\langle\overline{d}\,d\rangle$ are numbers, that have to be derived by phenomenological fits or computed from LQCD. Fortunately once found, the value of the condensate can be used for any process.

In summary we note that the usage of the OPE and its validity is far from obvious. Until today there is no analytic proof of the OPE. Furthermore we are deriving the OPE from matching the Wilson coefficients to Feynman graph analyses. These Feynman-graphs are calculated perturbatively but the coefficients with dimension $D > 0$ correspond to NP condensates! The condensates by themselves have to be gathered from external, NP methods.

Now that we have a tool to deal with the QCD vacuum and NPT effects we are left with two problems. First we still do not know how to deal with hadronic states in the quark-gluon picture. This will be tackled by duality. Secondly we have seen that we can access the two-point function theoretically on the physical sheet except for the positive real axis, due to its analytic properties. Unfortunately the experimental measurable spectral function is solely be defined on this positive real axis, which is theoretically not accessible. To match the theory with the experiment we will have to apply Cauchy's theorem. In the final section of this chapter we will bring together the two-point function, the OPE, duality and Cauchy's theorem to formulate the QCDSR.

## 2.4 Sum Rules

The QCDSR are a method to connect the DOF of QCD, the quarks and gluon fields, to the DOF of the vacuum spectrum of hadrons, thereby allowing for the determination of the strong coupling. To do so we have to treat the in **??** introduced two-point function NP with the help of the OPE

$$\Pi(s) \to \Pi_{\text{OPE}}(s). \qquad (2.4.1)$$

QCDSR furthermore introduce an ad hoc assumption, namely *quark-hadron duality*, stating that the observable hadron picture can be equally described by the QCD quark-gluon picture and that both pictures are equally valid. As the experimentally measured hadronic states are represented in poles and cuts on the positive real axis of the two-point function, which we have encountered in the analytic properties of its spectral decomposition, we will follow the prescription of QCDSR to apply *Cauchy's theorem* and weight functions to take care of perturbative complications close to the positive real axis.

### 2.4.1 The Dispersion Relation

We have already seen the Källén-Lehmann spectral representation in **??**. The general dispersion relation is defined to have an additional polynomial function $P(s)$

$$\Pi(s) = \int_0^\infty \frac{\rho(s')}{s' - s - i\epsilon} + P(s), \tag{2.4.2}$$

which accounts for the fact, that the two-point function increases for large $s$, but the integral on the RHS cannot reproduce this behaviour. For example the vector correlator carries only a constant and the scalar correlator a linear polynom. The two-point function is in general an unphysical quantity, whereas the spectral function $\rho(s)$ is a physical quantity. As a result the polynomial accounts carries the unphysical scale dependency of the two-point function.

### 2.4.2 Duality

QCD treats quarks and gluon as its fundamental DOF, but due to confinement we are only ever able to observe hadrons. The mechanism that connects the two worlds is the *quark-hadron duality* (or simply duality), which implies that physical quantities can be described equally good in the hadronic or in the quark-gluon picture. Thus we can connect experimental detected with theoretically calculated values from the two-point function in the dispersion relation **??** as

$$\Pi_{th}(s) = \int_0^\infty \frac{\rho(s')_{exp}}{s' - s - i\epsilon} + P(s), \tag{2.4.3}$$

where we connected the theoretical correlator $\Pi_{th}$ with the experimental measurable spectral function $\rho_{exp}$. We can represent duality as, substituting the two-point function **[Cata2005]**

$$\Pi(s) \to \Pi_{OPE}(s). \tag{2.4.4}$$

If this approximation carries no error, we would say that the experimental spectral function $rho_{exp}(s) = 1/\pi \, \mathrm{Im} \, \Pi(s)$ is dual to the OPE. On the contrary if the substitution is not exact we are missing contributions, which are represented by the so-called DV.

**Duality Violations**

There also exist situations where we cannot make use of duality. These situation are referred to as DV and belong to the non-perturbative part of the theory. It is often assumed that by applying the OPE to all orders we account for all non-perturbative effects, including DV. Unfortunately this assumption is only partly right. Even if we could compute the OPE to all orders, we would still experience discrepancies to our theoretical results. In general it is said, that if we have deviations beyond the natural uncertainty of the OPE we call them DV [**Shifman2000**]. E.g. if we compute $\Pi(s)$ to orders of $\alpha^2$ and $\frac{1}{Q^4}$, while we cutoff higher orders ($\alpha^3$ and $\frac{1}{Q^6}$), where $Q^2 \equiv -q^2$, then we get a natural error, because we have not calculated the full series. Values of the hadronic spectral density, out of range of the natural error, are then DV.

A detailed discussion of duality has been given by the author of the [**Shifman2000**].

### 2.4.3 Finite Energy Sum Rules

To theoretical calculate the two-point function we have to integrate the experimental data $\rho_{exp}(s)$ from 0 to infinity. No experiment will ever take data for an infinite momentum $s$. For $\tau$ decays we are limited to energies around the $\tau$ mass of 1.776 GeV. To deal with the upper integration limit several approaches have been made. One of them, the *Borel transformation*, is to exponentially suppress higher energy contributions (see [**Weinberg1996**, **Rafael1997**]). The technique we are using is called *finite energy sum rules* (FESR) and introduces

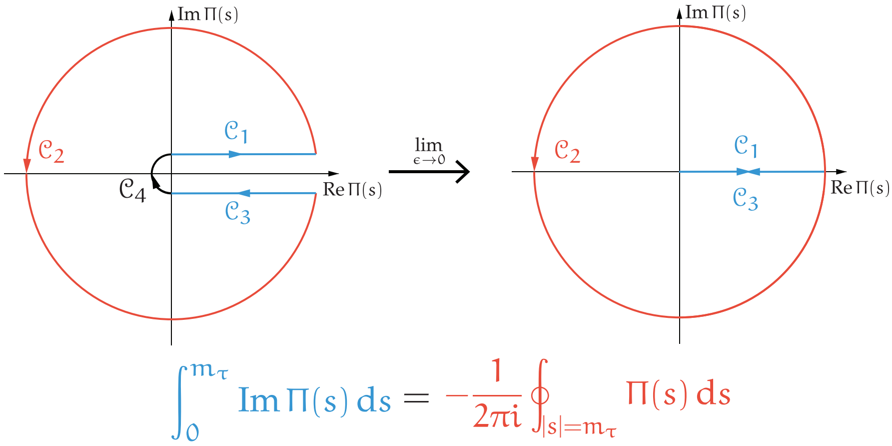


Figure 2.6: Visualisation of the usage of Cauchy's theorem to transform **??** into a closed contour integral over a circle of radius $s_0$.

a energy cut-off. We thus integrate the experimental data $\rho(s)$ only to a certain energy $s_0$. Furthermore we have to theoretically evaluate the integral over the spectral function of the dispersion relation (**??**), which includes singularities caused by the hadronic spectrum. As a result we have to apply Cauchy's theorem

$$\oint_{\mathcal{C}} f(z) = 0, \tag{2.4.5}$$

which states that any integral over an analytic function $f(z)$ on a closed contour $\mathcal{C}$ has to be zero. Thus we can construct a contour to avoid the positive problematic real axis. Pictorial the contour is drawn in **??** and mathematically we can express it as

$$\oint \Pi(s) = \int_0^{s_0} \Pi(s+i\epsilon) - \Pi(s-i\epsilon)\,ds + \int_{0+\alpha(\epsilon)}^{2\pi-\alpha(\epsilon)} \Pi(s_0 e^{i\theta})\,d\theta + \int_{3\pi/2}^{\pi/2} \Pi(\epsilon e^{i\theta})\,d\theta \tag{2.4.6}$$

If we make to use of *Schwartz reflection principle*:

$$f(\bar{z}) = \overline{f(z)}, \tag{2.4.7}$$

which can be applied if $f$ is analytic and maps only to real values on the positive real axis, we can express the integrand of the first integral of **??** as the imaginary part of the two-point function

$$\Pi(s+i\epsilon) - \Pi(s-i\epsilon) = \Pi(s+i\epsilon) - \Pi^*(s+i\epsilon) = 2i\operatorname{Im}\Pi(s+i\epsilon), \tag{2.4.8}$$

which is by definition equal to the spectral function

$$\rho(s) \equiv \frac{\operatorname{Im}\Pi(s)}{\pi}. \tag{2.4.9}$$

After taking the limit of small epsilon we can relate the line integral to a finite momentum $s_0$ experimental spectral function to a theoretical accessible circular contour integral of radius $s_0$

$$\int_0^{s_0} \rho(s) = \frac{-1}{2\pi i} \oint_{|s|=s_0} \Pi(s)\, ds, \quad \text{where we applied} \quad \epsilon \to 0. \tag{2.4.10}$$

Note that the unphysical contribution of the polynomial in **??** cancel in the contour integral.

We are free to multiply the upper equation with an analytic function $\omega(s)$, which completes the FESR

$$\int_0^{s_0} \omega(s)\rho(s) = \frac{-1}{2\pi i} \oint_{|s|=s_0} \omega(s)\Pi_{OPE}(s)\, ds \tag{2.4.11}$$

where the *left-hand side* (LHS) can be taken from experiment and the RHS by the theoretically evaluated correlator $\Pi_{OPE}(s)$. The analytic function $\omega(s)$ plays the role of a weight. It can be used to further suppress the non-perturbative contributions coming from *duality violations* (DV) and also enhance or suppress different contributions of the OPE as we will see.

### 2.4.4 Weighting OPE dimensions

We have seen that the perturbative part of the two-point function carries a discontinuity on the positive real axis. Consequently we applied Cauchy's theorem to avoid the not analytic part of the two point function. This left us with non-closed contour integral for the perturbative part of the OPE, which will always contribute. On the other hand, the strength of the higher dimension contributions of the OPE can modified. We can use different weights to control the dimensions of the OPE that contribute. The weights we are using have to be analytic, so that we can make use of Cauchy's theorem. Thus they can be represented as polynomials

$$\omega(x) = \sum_i a_i x^i, \tag{2.4.12}$$

every contributing monomial is responsible for a dimension of the OPE. Dimensions that are not represented in the weight polynomial do not contribute at all or are very suppressed as we will demonstrate now.

| **monomial:** | $x^0$ | $x^1$ | $x^2$ | $x^3$ | $x^5$ | $x^6$ | $x^7$ |
|---|---|---|---|---|---|---|---|
| **dimension:** | $D^{(2)}$ | $D^{(4)}$ | $D^{(6)}$ | $D^{(8)}$ | $D^{(10)}$ | $D^{(12)}$ | $D^{(14)}$ |

Table 2.3: List of monomial and their corresponding "active" dimensions in the OPE. Note that the perturbative contributions of the OPE are always present.

The residue of a monomial $x^k$ is only different from 0 if its power $k = -1$:

$$\oint_C x^k \, dx = i \int_0^{2\pi} \left(e^{i\theta}\right)^{k+1} d\theta = \begin{cases} 2\pi i & \text{if } k = -1, \\ 0 & \text{otherwise} \end{cases}. \tag{2.4.13}$$

Consequently if we exchange the *kinematic weight*

$$\omega_\tau(s) \equiv \left(1 - \frac{s}{m_\tau^2}\right)^2 \left(1 + 2\frac{s}{m_\tau^2}\right), \tag{2.4.14}$$

which we will see appears naturally in the inclusive $\tau$ decay ratio (**??**), through a monomial and neglect all terms of no interest to us we can write

$$\begin{aligned} R(xm_\tau)\big|_{D=0,2,4...} &= \oint_{|x|=1} dx \frac{x^k}{(xm_\tau)^{\frac{D}{2}}} C^D(xm_\tau) \\ &= \frac{1}{(m_\tau)^{\frac{D}{2}}} \oint_{|x|=1} dx x^{k-D/2} \, C^D(xm_\tau), \end{aligned} \tag{2.4.15}$$

where $C^D$ are the $D$-dimensional Wilson coefficients. Thus combining **??** with **??** we see that only Dimension which fulfil

$$k - D/2 = -1 \quad \Longrightarrow \quad D = 2(k+1) \tag{2.4.16}$$

contribute to the OPE. For example the polynomial of the kinematic weight is given by

$$(1-x)^2(1+2x) = \underbrace{1}_{D=2} - 3\underbrace{x^2}_{D=6} + 2\underbrace{x^3}_{D=8}, \tag{2.4.17}$$

where the underbraced monomials express the active dimensions. A list of monomials and their corresponding Dimensions up to dimension 14 can be found in **??**. This behaviour enables us to bring out different dimensions of the OPE and suppress contributions of higher order ($D \geqslant 10$ for which less is known.

For the interested reader we gathered several introduction texts to the QCDSR, which where of great use to us [**Narison1989**, **Rafael1997**, **Colangelo2000**, **Dominguez2013**].

Chapter 3

# Tau Decays into Hadrons

The $\tau$ lepton is an elementary particle with spin $1/2$ and as mass of $1.776\,86\,\mathrm{GeV}$ [**PDG2018**]. It is the only lepton heavy enough to decay into hadrons but also light enough for performing a low-energy QCD analysis. Its inclusive hadronic[1] decay ratio is given by

$$R_\tau = \frac{\Gamma(\tau \to \nu_\tau + \text{hadrons})}{\Gamma(\tau \to \nu_\tau e^- \overline{\nu_e})} \tag{3.0.1}$$

and sensible to the strong coupling, due to its rather large value, at the $m_\tau^2$ scale, of approximately 0.33. On the other hand $\alpha_s(m_\tau^2)$ is small enough to apply the OPE. The NP OPE contributions to the decay ratio are suppressed. The dimension two contribution of the OPE is proportional to the quark masses and has only a tiny contribution for light quarks. The dimension four contribution can be suppressed by applying weight functions, that do not have a monomial in $x$. E.g. the kinematic weight $\omega_\tau = (1-x)^2(1+2x) = 1-3x^2+2x^3$ is not sensitive to OPE corrections of dimension four. The dimension six contribution of the OPE is proportional to $1/(m_\tau^2)^3$ and further suppressed in the V+A channel of the vector and axial-vector $D=6$ contributions have opposite signs and partly cancel themselves. Higher dimensional OPE contributions are suppressed by terms $1/m_\tau^n$ with $n \geqslant 8$. As a result the perturbative contributions are dominant. They are known up to order $(\alpha_s^4)$ with a total contribution of 20% to $R_\tau$ [**Pich2016a**], which enables us to perform precise calculations of the inclusive $\tau$ decay ratio. Furthermore by extracting $\alpha_s$ at low energies at the scale of $m_\tau^2$ we will achieve lower errors for the strong coupling at higher energies as the errors run with the strong coupling and get smaller with increasing

[1] Meaning all decay channels with a hadron in its final state.

energy.

Summarising the $\tau$ decays permit one of the most precise determinations of the strong coupling $\alpha_s$. Building on the previously presented QCDSR we will now elaborate the needed theory to extract $\alpha_s$ from the process of hadronic tau decays.

## 3.1 The Inclusive Decay Ratio

The theoretical expression of the inclusive hadronic decay ratio (**??**) is given by

$$R_\tau(s) = 12\pi S_{EW}|V_{ud}|^2 \int_0^{m_\tau} \frac{ds}{m_\tau^2}\left(1-\frac{s}{m_\tau^2}\right)\left[\left(1+2\frac{s}{m_\tau^2}\right)\operatorname{Im}\Pi^{(1)}(s)+\operatorname{Im}\Pi^{(0)}(s)\right], \tag{3.1.1}$$

where $S_{EW}$ is the electroweak correction, $V_{ud}$ the corresponding *Cabibbo-Kobayashi-Maskawa* (CKM) matrix element and $\operatorname{Im}\Pi$ the imaginary part of the two-point function we introduced in **??**. For brevity we will omit the electroweak $S_{EW}$ and CKM factors from now on. **??** was first derived by [**Tsai1971**], using current algebra, a more recent derivation making use of the *optical theorem*, as already mentioned in **??** can be taken from [**Schwab2002**]. Notice that we used the standard Lorentz decomposition into transversal ($J = 1$) and longitudinal ($J = 0$) components of **??** to display the hadronic decay ratio (**??**).

Applying Cauchy's theorem, as seen in **??**, to the **??** we can rewrite the line integral into a closed contour integral

$$R_\tau = 6\pi i \oint_{s=m_\tau} \frac{ds}{m_\tau^2}\left(1-\frac{s}{m_\tau^2}\right)\left[\left(1+2\frac{s}{m_\tau^2}\right)\Pi^{(1)}(s)+\Pi^{(0)}(s)\right]. \tag{3.1.2}$$

It is convenient to work with a slightly different combination of transversal and longitudinal components $\Pi^{(1+0)}$, which has been defined in **??** and is free of kinematic singularities. As a result we can further rewrite the hadronic $\tau$ decay ratio into

$$R_\tau = 6\pi i \oint_{|s|=m_\tau} \frac{ds}{m_\tau^2}\left(1-\frac{s}{m_\tau^2}\right)^2\left[\left(1+2\frac{s}{m_\tau^2}\right)\Pi^{(1+0)}(s)-\left(\frac{2s}{m_\tau^2}\right)\Pi^{(0)}(s)\right]. \tag{3.1.3}$$

In the case of $\tau$ decays we only have to consider vector and axial-vector contributions of decays into up, down and strange quarks.

With **??** we have a suitable physical quantity that can be theoretically calculated as experimentally measured. By using the QCDSR we apply a closed contour integral of radius $s_0$. As a result we successfully avoided low energies at which the application of PT would be questionable. For example if we would choose a radius with the size of the $\tau$ mass $m_\tau \approx 1.78\,\mathrm{MeV}$ the strong coupling would have a perturbatively safe value of $\alpha_s(m_\tau^2) \approx 0.33$ [**Pich2016**]. Obviously we would benefit even more from a contour integral over a bigger circumference, but $\tau$ decays are kinematically limited by their mass. Nevertheless there are promising $e^+e^-$ annihilation data, which yield valuable inclusive decay ratio values up to $2\,\mathrm{GeV}$ [**Boito2018**][**Keshavarzi2018**].

### 3.1.1 Renormalisation Group Invariance

We have seen in **??**, that the two-point function is not a physical quantity, as the dispersion relation (**??**) contains a unphysical polynom. Luckily for the vector correlator, appearing in hadronic tau decays, the polynom is just a constant. Consequently we can take the derivative with respect to the momentum $s$ to derive a physical quantity from the two-point function:

$$D(s) \equiv -s\frac{d}{ds}\Pi(s). \tag{3.1.4}$$

$D(s)$ is called the *Adler function* and fulfils, as all physical quantities, the RGE (**??**). The Adler function commonly has separate definitions for the longitudinal plus transversal and the solely longitudinal contributions:

$$D^{(1+0)}(s) \equiv -s\frac{d}{ds}\Pi^{(1+0)}(s), \qquad D^{(0)}(s) \equiv \frac{s}{m_\tau^2}\frac{d}{ds}\left(s\Pi^{(0)}(s)\right). \tag{3.1.5}$$

The two-point functions in **??** can now be replaced with the help of partial integration

$$\int_a^b u(x)V(x)\,dx = \left[U(x)V(x)\right]_a^b - \int_a^b U(x)v(x)\,dx. \tag{3.1.6}$$

We will perform two separate the computations the two cases $(1+0)$ and $(0)$.

Starting by the transversal plus longitudinal contribution we get:

$$\begin{aligned}
R_\tau^{(1)} &= \frac{6\pi i}{m_\tau^2}\oint_{|s|=m_\tau^2} \underbrace{\left(1-\frac{s}{m_\tau^2}\right)^2\left(1+2\frac{s}{m_\tau^2}\right)}_{=u(x)}\underbrace{\Pi^{(1+0)}(s)}_{=V(x)} \\
&= \frac{6\pi i}{m_\tau^2}\left\{\left[-\frac{m_\tau^2}{2}\left(1-\frac{s}{m_\tau^2}\right)^3\left(1+\frac{s}{m_\tau^2}\right)\Pi^{(1+0)}(s)\right]_{|s|=m_\tau^2}\right. \\
&\quad \left. +\oint_{|s|=m_\tau^2}\underbrace{-\frac{m_\tau^2}{2}\left(1-\frac{s}{m_\tau^2}\right)^3\left(1+\frac{s}{m_\tau^2}\right)}_{=U(x)}\underbrace{\tfrac{d}{ds}\Pi^{(1+0)}(s)}_{=v(x)}\right\} \\
&= -3\pi i\oint_{|s|=m_\tau^2 s}\frac{ds}{s}\left(1-\frac{s}{m_\tau^2}\right)^3\left(1+\frac{s}{m_\tau^2}\right)\tfrac{d}{ds}D^{(1+0)}(s)
\end{aligned} \tag{3.1.7}$$

where we fixed the integration constant to $c=-\frac{m_\tau^2}{2}$ in the second line and left the antiderivatives contained in the squared brackets untouched. If we parametrise the integral appearing in the expression in the squared brackets we can see that it vanishes:

$$\left[-\frac{m_\tau^2}{2}\left(1-e^{-i\phi}\right)^3\left(1+e^{-i\phi}\right)\Pi^{(L+T)}(m_\tau^2 e^{-i\phi})\right]_0^{2\pi}=0, \tag{3.1.8}$$

where $s\to m_\tau^2 e^{-i\phi}$ and $(1-e^{-i\cdot 0})=(1-e^{-i\cdot 2\pi})=0$. Repeating the same calculation for the longitudinal part yields

$$\begin{aligned}
R_\tau^{(0)} &= \oint_{|s|=m_\tau^2} ds\left(1-\frac{s}{m_\tau^2}\right)^2\left(-\frac{2s}{m_\tau^2}\right)\Pi^{(0)}(s) \\
&= -4\pi i\oint\frac{ds}{s}\left(1-\frac{s}{m_\tau^2}\right)^3 D^{(0)}(s)
\end{aligned} \tag{3.1.9}$$

Consequently combining the transversal with the longitudinal contribution results in

$$R_\tau = -\pi i\oint_{|s|=m_\tau^2}\frac{ds}{s}\left(1-\frac{s}{m_\tau^2}\right)^3\left[3\left(1+\frac{s}{m_\tau^2}D^{(1+0)}(s)+4D^{(0)}(s)\right)\right]. \tag{3.1.10}$$

It is convenient to define $x=s/m_\tau^2$ such that we can rewrite the inclusive ratio as

$$R_\tau = -\pi i\oint_{|s|=m_\tau^2}\frac{dx}{x}(1-x)^3\left[3(1+x)D^{(1+0)}(m_\tau^2 x)+4D^{(0)}(m_\tau^2 x)\right], \tag{3.1.11}$$

which will be the final expression we will be using to express the inclusive tau decay ratio.

## 3.2 Theoretical computation of $R_\tau$

The previously derived expression for the tau decay ratio is at first approximation equal to the number of colours **[Peskin1995]**

$$R_\tau \approx N_c. \tag{3.2.1}$$

If we take into account the perturbative $\delta_{pt}$ and non-perturbative $\delta_{npt}$ we can organise the vector and axial-vector inclusive decay ratio as

$$R^{\omega}_{\tau,V/A} = \frac{N_c}{2}\left(1 + \delta^{\omega}_{pt} + \delta^{\omega}_{npt}\right). \tag{3.2.2}$$

Note that the factor $1/2$ comes from the fact, that in the chiral limit the vector and axial-vector contributions are equal. The dependence on the chosen weight function $\omega$ is reflected in the upper indices.

For the kinematic weight

$$\omega_\tau \equiv (1-x)^2(1+2x), \tag{3.2.3}$$

we have a dominant perturbative contribution of $\delta_{pt} \approx 20\%$ to $R_\tau$ **[Pich2013]** and a minor, but not negligible, non-perturbative contribution of $\delta^{NP}_{V+A} \lesssim 1\%$ **[Jamin2013]** for the $V+A$-channel

In the following we want to derive the theoretical expressions needed to calculate both of the corrections to **??** starting with the perturbative one.

### 3.2.1 The perturbative contribution

The perturbative contribution $\delta_{pt}$ to the inclusive $\tau$ decay ratio is corresponds to the first term of the OPE. Currently the perturbative expansion has been calculated to fourth order $\mathcal{O}(\alpha_s^4)$. Due to their role as dominant corrections their uncertainties from unknown higher-order corrections dictate the final error of the determination of the strong coupling **[Pich2016]**.

We will treat the correlator in the chiral limit, in which the scalar and pseudoscalar contribution of the two-point function vanish and the axial and vectorial contributions are equal. As a result we can focus ourselves on the vector correlator $\Pi_V(s)$, which can be expanded as a sum over different orders of $\alpha$

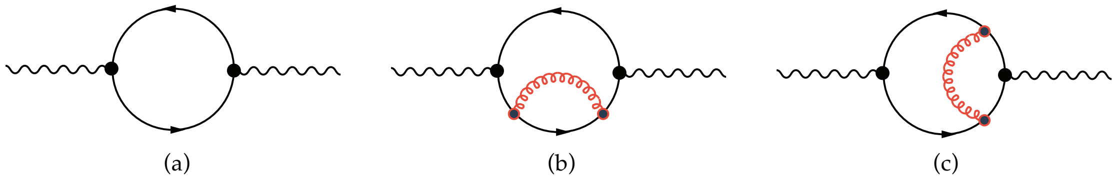

Figure 3.1: Feynman loop diagrams to calculate the $c_{n,k}$ coefficients of the expanded correlator $\Pi_V^{(1+0)}$. The internal red lines represent gluons. Diagram a) represents the parton model and diagrams b) and c) represent higher order corrections.

**[Beneke2008]**:

$$\Pi_V^{(1+0)}(s) = -\frac{N_c}{12\pi^2}\sum_{n=0}^{\infty} a_\mu^n \sum_{k=0}^{n+1} c_{n,k} L^k \quad \text{with} \quad L \equiv \ln\frac{-s}{\mu^2}, \tag{3.2.4}$$

where we defined $a_\mu \equiv \alpha(\mu)/\pi$. The coefficient $c_{n,k}$ up to two-loop order can be obtained by Feynman diagram calculations. With the diagrams of **??** we can calculate the one-loop result of the correlator **[Jamin2006]**

$$\Pi^B(q^2)\Big|^{1-\text{loop}} = \frac{N_c}{12\pi^2}\left(\frac{1}{\hat{\epsilon}} - \log\frac{(-q^2 - i0)}{\mu^2} + \frac{5}{3} + \mathcal{O}(\epsilon)\right), \tag{3.2.5}$$

where $\Pi^B_{\mu\nu}(q^2)$ is the bare two-point function [2]. This result can then be used to extract the first two coefficients of the correlator expansion given in **??**

$$c_{00} = -\frac{5}{3} \qquad \text{and} \qquad c_{01} = 1. \tag{3.2.6}$$

The second loop can also be calculated by diagram techniques resulting in **[Boito2011]**

$$\Pi_V^{(1+0)}(s)\Big|^{2-\text{loop}} = -\frac{N_c}{12\pi^2} a_\mu \log(\frac{-s}{\mu^2}) + \cdots \tag{3.2.7}$$

yielding $c_{11} = 1$.

Beginning from three loop diagrams the algebra becomes exhausting and one has to use dedicated algorithms to compute the higher loops. The third loop calculations have been done in the late seventies by **[Chetyrkin1979, Dine1979, Celmaster1979]**. The four loop evaluation have been completed a little more than ten years later by **[Gorishnii1990, Surguladze1990]**. The highest loop

[2] The term $1/\hat{\epsilon}$, which is of order zero in $\alpha_s$, is not present in the Adler function or the imaginary part of the correlator.

published, that amounts to $\alpha_s^4$, was published in 2008 [**Baikov2008**] almost 20 years later.

Fixing the number of colors to $N_c = 3$ the missing coefficients up to order four in $\alpha_s$ read:

$$\begin{aligned}
c_{2,1} &= \frac{365}{24} - 11\zeta_3 - \left(\frac{11}{12} - \frac{2}{3}\zeta_3\right) N_f \\
c_{3,1} &= \frac{87029}{288} - \frac{1103}{4}\zeta_3 + \frac{275}{6}\zeta_5 \\
&- \left(\frac{7847}{216} - \frac{262}{9}\zeta_3 + \frac{25}{9}\zeta_5\right) N_f + \left(\frac{151}{162} - \frac{19}{27}\zeta_3\right) N_f^2 \\
c_{4,1} &= \frac{78631453}{20736} - \frac{1704247}{432}\zeta_3 + \frac{4185}{8}\zeta_3^2 + \frac{34165}{96}\zeta_5 - \frac{1995}{16}\zeta_7,
\end{aligned} \tag{3.2.8}$$

where used the flavor number $N_f = 3$ for the last line.

The 6-loop calculation has until today not been computed, but Beneke and Jamin [**Beneke2008**] used and educated guess to estimate the coefficient

$$c_{5,1} \approx 283 \pm 283. \tag{3.2.9}$$

We often see $c_{5,1}$ applied to estimate the perturbative errors related to missing higher order contributions.

In stating the coefficients $c_{n,k}$ of the correlator expansion we have restricted ourselves to $k$ indices equal to one. This is due to the RGE, which relates coefficients with $k$ different than one to coefficients with $k$ equal to one ($c_{n,1}$). Consequently the correlator $\Pi_V^{1+0}(s)$ needs to be a physical quantity, which we can be achieved with the previously defined Adler function (**??**). The correct expression for the correlator expansion in **??** is then given by

$$D_V^{(1+0)} = -s\frac{d\Pi_V^{(1+0)}(s)}{ds} = \frac{N_c}{12\pi^2}\sum_{n=0}^{\infty} a_\mu^n \sum_{k=1}^{n+1} k c_{n,k} L^{k-1}, \tag{3.2.10}$$

where we used $dL^k/ds = k\ln(-s/\mu^2)^{k-1}(-1/\mu^2)$. Applying the RGE (**??**) to the scale-invariant Adler function yields

$$-\mu\frac{d}{d\mu}D_V^{(1+0)} = -\mu\frac{d}{d\mu}\left(\tfrac{\partial}{\partial L}\,dL + \tfrac{\partial}{\partial a_s}\,da_s\right) D_V^{(1+0)} = \left(2\tfrac{\partial}{\partial L} + \beta\tfrac{\partial}{\partial a_s}\right) D_V^{(1+0)} = 0, \tag{3.2.11}$$

where we made use of the $\beta$ function, which is defined in **??**, and of the expression $dL/d\mu = -2/\mu$.

The relation between the correlator expansion coefficients can then be taken by calculating the Adler function for a desired order and plugging it into the RGE. For example the Adler function to the second order in $\alpha_s$

$$D(s) = \frac{N_c}{12\pi^2}\left[c_{01} + a_\mu(c_{11} + 2c_{12}L) + a_\mu^2(c_{21} + 2c_{22}L + 3c_{23}L^2)\right], \quad (3.2.12)$$

can be inserted into the **??**

$$4a_\mu c_{12} + 2a_\mu^2(2c_{22} + 6c_{23}L) + \beta_1 a_\mu^2(c_{11} + 2c_{12}L) + \mathcal{O}(a_\mu^3) = 0 \quad (3.2.13)$$

to compare the coefficients order by order in $\alpha_s$. At order $\alpha_\mu$ only the $c_{12}$ term is present and has consequently to be zero. For $\mathcal{O}(a_\mu^2 L)$ solely $c_{23}$ exists as $c_{12} = 0$ and thus also has to vanish. Finally for $\mathcal{O}(a)$ we can relate $c_{22}$ with $c_{11}$ resulting in:

$$c_{12} = 0, \quad c_{22} = \frac{\beta_1 c_{11}}{4} \quad \text{and} \quad c_{23} = 0. \quad (3.2.14)$$

Implementing the newly obtained Adler coefficients we can write out the Adler function to the first order:

$$D(s) = \frac{N_c}{12\pi^2}\left[c_{01} + c_{11}a_\mu\left(c_{21} - \frac{1}{2}\beta_1 c_{11} L\right)a_\mu^2\right] + \mathcal{O}(a_\mu^3). \quad (3.2.15)$$

We have used the RGE to relate Adler function coefficients and thus only need to know coefficients of type $c_{n,1}$. Unfortunately, as we will see in the following section the RGE gives us two different choices in the order of the computation of the perturbative contribution to the inclusive tau decay ratio.

### Renormalization group summation

By making use of the RGE we have to decide about the order of mathematical operations we perform. As the all order perturbative contribution $\delta_{pt}$ is independent on the scale $\mu$ we are confronted with two choices: *fixed-order perturbation theory* (FOPT) and *contour-improved perturbation theory* (CIPT). Each of them yields a different result, which is the main source of error in extracting the strong coupling from tau decays.

Working in the chiral limit additionally permits us to neglect the longitudinal contribution $D^{(0)}$, in **??** of the perturbative contribution $\delta_{pt}$ of $R_\tau$ (**??**). Thus inserting the expansion of $D_V^{(1+0)}$ into the hadronic tau decay width **??** yields

$$\delta_{pt} = \sum_{n=1}^{\infty} a_\mu^n \sum_{k=1}^{n} k c_{n,k} \frac{1}{2\pi i}\oint_{|x|=1} \frac{dx}{x}(1-x)^3(1+x)\log\left(\frac{-m_\tau^2 x}{\mu^2}\right)^{k-1}, \quad (3.2.16)$$

where we kept in mind that the contributions from the vector and axial-vector correlator are identical in the massless case.

To continue evaluating the perturbative part we can now either follow the description of FOPT or CIPT. We will now present both.

In FOPT we fix the scale at the tau mass ($\mu^2 = m_\tau^2$), which leaves us with the integration over the logarithm, as seen in

$$\delta_{\mathrm{FO}}^{(0)} = \sum_{n=1}^{\infty} a(m_\tau^2)^n \sum_{k=1}^{n} k c_{n,k} J_{k-1} \tag{3.2.17}$$

where the contour integrals $J_l$ are defined by

$$J_l \equiv \frac{1}{2\pi i} \oint_{|x|=1} \frac{dx}{x} (1-x)^3 (1+x) \log^l(-x). \tag{3.2.18}$$

The integrals $J_l$ up to order $\alpha_s^4$ are given by [**Beneke2008**]:

$$J_0 = 1, \quad J_1 = -\frac{19}{12} \quad J_2 = \frac{265}{72} - \frac{1}{3}\pi^2, \quad J_3 = -\frac{3355}{288} + \frac{19}{12}\pi^2. \tag{3.2.19}$$

Using FOPT the strong coupling $a(\mu)$ is fixed at the tau mass scale $a(m_\tau^2)$ and can be taken out of the closed-contour integral. Thus we solely have to integrate over the logarithms $\log(x)$.

Using CIPT, on the contrary, we can sum the logarithms by setting the scale to $\mu^2 = -m_\tau^2 x$ in **??**, resulting in:

$$\delta_{\mathrm{CI}}^{(0)} = \sum_{n=1}^{\infty} c_{n,1} J_n^a(m_\tau^2), \tag{3.2.20}$$

where the contour integrals $J_l$ are defined by

$$J_n^a(m_\tau^2) \equiv \frac{1}{2\pi i} \oint_{|x|=1} \frac{dx}{x} (1-x)^3 (1+x) a^n(-m_\tau^2 x). \tag{3.2.21}$$

Note that all logarithms vanish, except the ones with index $k = 1$:

$$\log(1)^{k-1} = \begin{cases} 1 & \text{if } k = 1, \\ 0 & k \neq 1 \end{cases} \tag{3.2.22}$$

which selects the Adler function coefficients $c_{n,1}$. Handling the logarithms left us with the integration of the strong coupling $\alpha_s(-m_\tau^2 x)$ over the closed-contour $\oint_{|x|=1}$, which now depends on the integration variable $x$.

In general we have to decide if we want to perform a contour integration with a constant strong coupling parameter and variable logarithms (FOPT) or "constant logarithms" and a running coupling (CIPT). To emphasize the differences in both approaches we can calculate the perturbative contribution $\delta^{(0)}$ to $R_\tau$ for the two different prescriptions yielding [**Beneke2008**]

$$\begin{aligned}
&\qquad\quad \alpha_s^2 \qquad\; \alpha_s^2 \qquad\; \alpha_s^3 \qquad\; \alpha_s^4 \qquad\quad\;\; \alpha_s^5 \\
\delta^{(0)}_{FO} &= 0.1082 + 0.0609 + 0.0334 + 0.0174(+0.0088) = 0.2200(0.2288) \qquad (3.2.23)\\
\delta^{(0)}_{CI} &= 0.1479 + 0.0297 + 0.0122 + 0.0086(+0.0038) = 0.1984(0.2021). \qquad (3.2.24)
\end{aligned}$$

The series indicate, that CIPT converges faster and that both series approach a different value. This discrepancy represents currently the biggest theoretical uncertainty for extracting the strong coupling.

As today FOPT or CIPT are equally valid approaches to calculate the perturbative contributions. As a result there are currently three ways of stating results: Quoting the average of both results, quoting the CIPT result or quoting the FOPT result. We follow the approach of Beneke and Jamin [**Beneke2008**] who prefere FOPT, but also state their results in CIPT.

### 3.2.2 The Non-Perturbative OPE Contributions

The perturbative contribution to the sum rule is the dominant one, but NP have to be taken into account. The contribution of the NP part can be quoted as [**Jamin2013**]

$$\delta^{NP}_{V+A,FO} = -0.086(80), \qquad \delta^{NP}_{V+A,CI} = 0.0089(65) \qquad (3.2.25)$$

which is small, but not negligible. The NP OPE contributions are commonly categorised by even, increasing dimensions. Contributions of dimension larger than eight are normally neglected, due to the increasing suppression by factors of $1/m_\tau^{2\cdot D}$, where D stands for the corresponding dimension.

The dimension two contributions are proportional to the quark masses and vanish while working in the chiral limit. Consequently we will neglect them and start by stating the $D = 4$ contributions.

### 3.2.3 Dimension Four

The next apparent OPE contribution is of dimension four. Here we have to take into account the terms with masses to the fourth power ($m^4$), the quark condensate multiplied by a mass ($m\langle\overline{q}\,q\rangle$) and the gluon condensate ($\langle GG\rangle$). The resulting expression can be taken from the appendix of [**Pich1999**], yielding:

$$D_{ij}^{(1+0)}(s)\Big|_{D=4} = \frac{1}{s^2}\sum_n \Omega^{(1+0)}(s/\mu^2)a^n, \tag{3.2.26}$$

where

$$\begin{aligned}\Omega_n^{(1+0)}(s/\mu^2) \;=\; & \frac{1}{6}\langle aGG\rangle p_n^{(1+0)}(s/\mu^2) + \sum_k m_k\langle\overline{q}_k q_k\rangle r_n^{(1+0)}(s/\mu^2) \\ & + 2\langle m_i\overline{q}_i q_i + m_j\overline{q}_j q_j\rangle q_n^{(1+0)}(s/\mu^2) \pm \frac{8}{3}\langle m_j\overline{q}_i q_i + m_i\overline{q}_j q_j\rangle t_n^{(1+0)} \\ & - \frac{3}{\pi^2}(m_i^4 + m_j^4)h_n^{(1+0)}(s/\mu^2) \mp \frac{5}{\pi^2}m_i m_j(m_i^2 + m_j^2)k_n^{(1+0)}(s/\mu^2) \\ & + \frac{3}{\pi^2}m_i^2 m_j^2 g_n^{(1+0)}(s/\mu^2) + \sum_k m_k^4 j_n^{(1+0)}(s/\mu^2) + 2\sum_{k\neq l} m_k^2 m_l^2 u_n^{(1+0)}(s/\mu^2)\end{aligned} \tag{3.2.27}$$

The perturbative expansion coefficients are known to second order $\mathcal{O}(a^2)$ for the condensate contributions,

$$\begin{array}{llll} p_0^{(1+0)} = 0, & p_1^{(1+0)} = 1, & p_2^{(1+0)} = \frac{7}{6}, \\ r_0^{(1+0)} = 0, & r_1^{(1+0)} = 0, & r_2^{(1+0)} = -\frac{5}{3} + \frac{8}{3}\zeta_3 - \frac{2}{3}\log(s/\mu^2), \\ q_0^{(1+0)} = 1, & q_1^{(1+0)} = -1, & q_2^{(1+0)} = -\frac{131}{24} + \frac{9}{4}\log(s/\mu^2) \\ t_0^{(1+0)} = 0 & t_1^{(1+0)} = 1, & t_2^{(1+0)} = \frac{17}{2} + \frac{9}{2}\log(s/\mu^2). \end{array} \tag{3.2.28}$$

while the $m^4$ terms have been only computed to first order $\mathcal{O}(a)$

$$\begin{array}{ll} h_0^{(1+0)} = 1 - 1/2\log(s/\mu^2), & h_1^{(1+0)} = \frac{25}{4} - 2\zeta_3 - \frac{25}{6}\log(s/\mu^2) - 2\log(s/\mu^2)^2, \\ k_0^{(1+0)} = 0, & k_1^{(1+0)} = 1 - \frac{2}{5}\log(s/\mu^2), \\ g_0^{(1+0)} = 1, & g_1^{(1+0)} = \frac{94}{9} - \frac{4}{3}\zeta_3 - 4\log(s/\mu^2), \\ j_0^{(1+0)} = 0, & j_1^{(1+0)} = 0, \\ u_0^{(1+0)} = 0, & u_1^{(1+0)} = 0. \end{array} \tag{3.2.29}$$

The above condensates all depend on the scale $\mu^2$, but we can express them in form of the scale-invariant gluon-and quark-condensate [**Spiridonov1988**], which are combinations of the minimally subtracted operators

$$\beta_1 \langle aG^2 \rangle_I \equiv \beta(s) \langle G^{\mu\nu}_{(a)} G^{(a)}_{\mu\nu} \rangle + 4\gamma(a) \sum_{i=u,d} \langle m_i \bar{q}_i q_i \rangle$$
$$- \frac{3}{4\pi^2} \sum_{i,j=u,d} m_i^2 m_j^2 \gamma_0^{ij}(a) \tag{3.2.30}$$
$$\langle m_i \bar{q}_j q_j \rangle \equiv \langle \bar{q}_j q_j \rangle + \frac{3m_i m_j^3}{7\pi^2 a} \left\{ 1 - \frac{53}{24} a + \mathcal{O}(a^2) \right\}, \tag{3.2.31}$$

where $\gamma_0^{ij}(a) = -2 - 8/3a$. During this work we will insert the known invariant quark condensates (see **??**) as constants and state our results for the invariant gluon condensate.

### 3.2.4 Dimension Six and Eight

Our application of dimension six contributions is founded in [**Braaten1991**] and has previously been calculated beyond leading order by [**Lanin1986**]. The operators appearing are the masses to the power six ($m^6$), the four-quark condensates ($\langle \bar{q} q \bar{q} q \rangle$), the three-gluon condensates ($\langle g^3 G^3 \rangle$) and lower dimensional condensates multiplies by the corresponding masses, such that in total the mass dimension of the operator will be six. The largest contributions comes from the 4-quark operators. The three-gluon condensate does not contribute at leading order [**Hubschmid1982**] and is neglected. Operators proportional to the light quark masses will also be neglected. The resulting contribution of dimension six operators has been calculated in [**Laning1986**] and leads to a large amount of operators, which until today cannot be accurately determined by phenomenology methods. To reduce the number of operators we can make use of the *vacuum saturation approach* (VSA) [**Beneke2008**, **Braaten1991**, **Shifman1978**] to express them in quark condensates $\langle q\bar{q} \rangle$. For Wilson coefficients of order $\alpha_s$ and applying the vacuum saturation we get a dimension six contributions of

$$D^{1+0}_{ij,V/A}(s)\Big|_{D=6} = \frac{32\pi^2}{3} a(\mu) \frac{\langle \bar{q}_i q_i(\mu) \rangle \langle \bar{q}_j q_j \rangle}{s^3} - \frac{32}{7} \pi^2 a_\mu \frac{\langle \bar{q}_i q_i \rangle^2 \langle \bar{q}_j q_j \rangle^2}{s^3}. \tag{3.2.32}$$

Unfortunately the scaling properties of the dimension six contribution, resulting from the VSA, are inconsistent with the scaling properties of the 4-quark operators [**Narison1983**, **Jamin1985**] and terms of order $\alpha_s^2$ are usually ignored.

In addition to the scaling problematic the VSA is known to underestimate the dimension six contribution [**Launer1983**].

In our work we take the simplest approach possible: Introducing an effective dimension six coefficient $\rho^{(6)}_{V/A}$ divided by the appropriate power in s

$$D^{(1+0)}_{ij,V/A}(s)\Big|_{D=6} = 3\frac{\rho^{(6)}_{V/A}}{s^3} \tag{3.2.33}$$

Here we also neglected the scale dependence of the dimension six operator, which is determined by the anomalous dimension, similar to the mass anomalous dimension given in **??**. We have calculated the leading-order anomalous dimension matrices corresponding to the dimension-6 four-quark operators of flavour non-diagonal, as well as flavour diagonal, mesonic vector and axial-vector currents in [**Boito2015**].

As for the dimension eight contribution the situation is not better than the dimension six one we keep the simplest approach, leading to

$$D^{(1+0)}_{ij,V/A}\Big|_{D=8} = 4\frac{\rho^{(8)}_{V/A}}{s^4}. \tag{3.2.34}$$

The NP contribution of dimension eight is the highest order that we are going to implement. Higher orders will be neglected. Next to the NP treatment of the OPE we have to discuss possible duality violations.

## 3.3 Duality Violations

As seen in **??** we have to assume quark-hadron duality for the QCDSR to work. Unfortunately duality is always to some extend broken through so-called *duality violations* (DV), which are well known [**Cata2008**, **Cata2009**]. Experimental data show an oscillating behaviour that cannot be reproduced by the OPE. Moreover in the large $N_c$ limit it can be shown that DV have an exponential decreasing, sinusoidal appearance [**Cata2005**]. Consequently for the cases with apparent DV we have to somehow include the corrections coming from DV and adapt **??**, leading to

$$R^{\omega}_{\tau,V/A} = \frac{N_c}{2} S_{EW} |V_{ud}|^2 \left(1 + \delta^{\omega}_{pt} + \delta^{\omega}_{npt} + \delta^{\omega}_{dv}\right), \tag{3.3.1}$$

where we extracted $\delta_{dv}$ from $\delta_{npt}$, even though DV are an NP. The DV correction has been modelled [**Cata2009**] with the following ansatz

$$\rho^{DV}_{V/A}(s) = e^{-(\delta_{V/A}+\gamma_{V/A}s)}\sin(\alpha_{V/A}+\beta_{V/A}s). \tag{3.3.2}$$

Here the DV contributions have been parametrised by four parameters for the vector and another four parameters for the axial-vector contribution. Note that for fitting the kinematic weight in the V-channel, which is known to be sensible for DV at lower energies [**Boito2011a**], we would have seven parameters instead of only three. Making use of the model (**??**) the DV then appear as an additional term in the inclusive tau decay ratio

$$R_{\tau,V/A} = -\pi i \oint_{|s|=m_\tau^2} \frac{dx}{x}(1-x)^3\left[3(1+x)D^{(1+0)}(m_\tau^2 x) + 4D^{(0)}(m_\tau^2 x)\right] + \mathcal{D}_{V/A}(m_\tau^2), \tag{3.3.3}$$

where the DV would be given as

$$\mathcal{D}_\omega(m_\tau^2) = -12\pi^2\int_{m_\tau^2}^{\infty}\frac{ds}{m_\tau^2}\omega(s)\rho_{V/A}. \tag{3.3.4}$$

### 3.3.1 Pinched weights to avoid DVs

The general QCDSR (**??**) contain a weight function $\omega$, which is used to weight higher order dimensions, but also to suppress DV. The weights that suppress DV are so-called pinched weights of the form

$$\omega(s) = \left(1-\frac{s}{m_\tau^2}\right)^k, \tag{3.3.5}$$

where $k$ is the degree of the pinched weight. The higher the degree of the pinching, the lower the suppression of the critical region close to the real axis (see. **??**). Thus for higher pinchings we are better protected from DV effects. For the transversal component of the inclusive tau decay ratio (**??**) a pinching of second degree appears quite naturally as the kinematic weight (see **??**). In general it is said that a double pinched weight is sufficient to neglect effects caused by DV. In our analysis we show that double pinched weights indeed sufficiently suppress DV and that even single pinched weights yield acceptable results. Additionally to applying pinched weights we focus on combinations of vector and axial-vector contributions, which as we will see now have visibly suppressed DV.

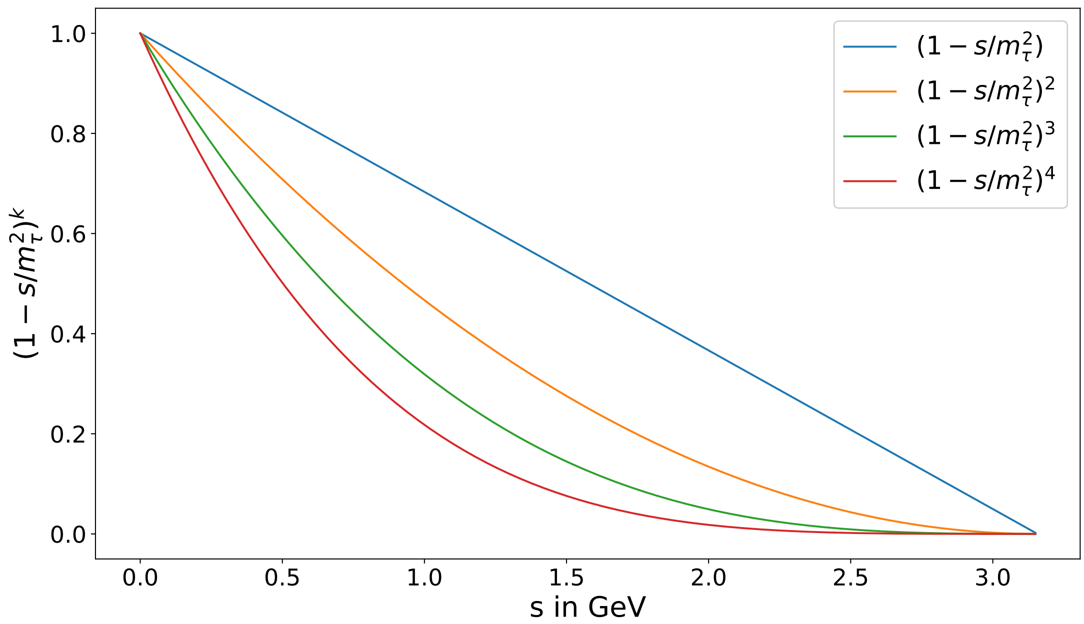


Figure 3.2: Pinched weights $(1 - s/m_\tau^2)^k$ for degrees 1 to 4. We can see that weights of higher pinching decrease faster, which comes in handy if we want to suppress duality violations.

## 3.4 Experiment

The tau decay data we use to perform our QCD analysis is from the ALEPH experiment. The ALEPH experiment was located at the *large-electron-positron* (LEP) collider at *European Organisation for Nuclear Research* (CERN) in Geneva. LEP started producing particles in 1989 and was replaced in the late 90s by the *large-hadron-collider* (LHC), which makes use of the same tunnel of 27 km circumference. The data produced within the experiment is still maintained by former ALEPH group members led by M. Davier, which have performed regular updates on the data-sets [**Davier2013**, **Davier2008**, **Aleph2005**]. The last update was motivated by Boito et al. [**Boito2010**], who discovered irregularities in the covariances by comparing data from a Monte Carlo generator with the ALEPH.

The measured spectral functions for the ALEPH data are defined in [**Davier2007**] and given for the transverse and longitudinal components separately

$$\rho^{(1)}_{V/A}(s) = \frac{m_\tau^2}{12|V_{ud}|^2\,S_{EW}} \frac{\mathcal{B}(\tau^- \to V^-/A^-\nu_\tau)}{\mathcal{B}(\tau^- \to e^-\overline{\nu}_e\nu_\tau)} \times \frac{dN_{V/A}}{N_{V/A}\,ds}\left[\left(1-\frac{s}{m_\tau^2}\right)^2\left(1+\frac{2s}{m_\tau^2}\right)\right]^{-1} \tag{3.4.1}$$

$$\rho^{(0)}_{A}(s) = \frac{m_\tau^2}{12|V_{ud}|^2\,S_{EW}} \frac{\mathcal{B}(\tau^- \to \pi^-(K^-)\nu_\tau)}{\mathcal{B}(\tau^- \to e^-\overline{\nu}_e\nu_\tau)} \times \frac{dN_A}{N_A\,ds}\left(1-\frac{s}{m_\tau^2}\right)^{-2}.$$

The data relies on a separation into vector and axial-vector channels. In the case of the $\pi$ this can be achieved via counting. The vector channel is characterised by a negative G-parity, whereas the axial-vector channel has positive G-parity. A single $\pi$ carries negative G-parity, an even number of $\pi$ carries positive G-parity and an odd number of $\pi$ carries negative G-parity:

$$n \times \pi = \begin{cases} \text{vector} & \text{if } n \text{ is even,} \\ \text{axial-vector} & \text{otherwise} \end{cases}. \tag{3.4.2}$$

The separation into vector and axial-vector channel of mesons including strange quarks, like $K\overline{K}$ pairs, is more difficult, because these are not in general eigenstates of G-parity and contribute to both V and A channels.

The contributions to the spectral function for the vector, axial-vector and V+A channel can be seen in **??**. The dominant modes in the vector case are **[Davier2006]** decays into two ($\tau^- \to \pi^-\pi^0\nu_\tau$) or four ($\tau^- \to \pi^-\pi^-\pi^+\pi^0\nu_\tau$) pions. The first of these is produced by an intermediate $\rho(770)$ meson, which in contrary to the pions carries angular momentum of one and clearly visible as peak around 770 GeV in **??**. The dominant modes in the axial-vector case are decays into one ($\tau^- \to \pi^-\nu_\tau$) or three ($\tau^- \to \pi^-\pi^0\pi^0\nu_\tau$ and $\tau^- \to \pi^-\pi^-\pi^+\nu_\tau$) pions. Here the three pion final states stem from the $a_1^-$-meson, which can be seen as a peak in **??**.

We furthermore added the perturbative contribution for a fixed $\alpha_s(m_\tau) = 0.329$ using FOPT in **??**. We can see, that the perturbative contribution (the blue line) is an almost straight line and cannot reproduce the oscillating behaviour, given by the ALEPH data. This is especially the case for the V and A channel and is seen as an indicator for DV. Even including NP, higher dimensions of the OPE is not reproducing the wavy structure. In the case of V+A, we have an higher agreement between our perturbative graph and the data. In general we believe

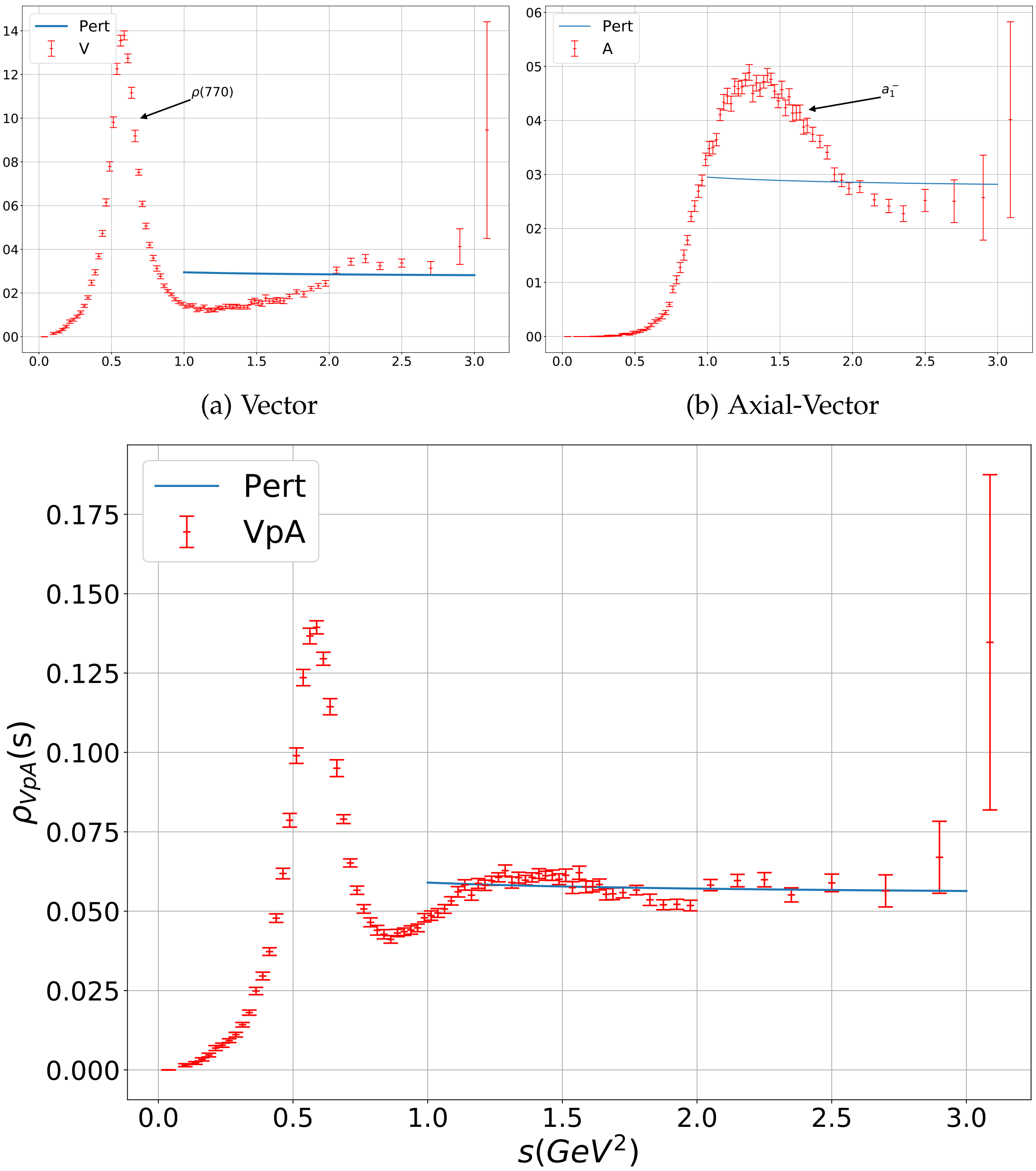


(a) Vector

(b) Axial-Vector

(c) Vector plus Axial-Vector

Figure 3.3: Visualisation of the vector, axial-vector and V+A spectral function given by the ALEPH data **[Davier2013]** in red with errors. We also plotted the FOPT theoretical calculation up to third order in $\alpha_s$, for a fixed $\alpha_s(\tau) = 0.329$ in blue. Note that the perturbative contribution can only limited represent the experimental data. It does not reproduce the sinusoidal form.

that DV are sufficiently suppressed in the case of V+A and will argument in favour of this statement in the following chapter. This is only the case for energies larger than 1.5 GeV, as the $\rho$ resonance of the V channel is impossible to be represented by perturbative tools. For lower energies DV become too important to be neglected.

### 3.4.1 Total decay ratio from experimental data

The data has been last revised in 2014 [**Davier2014**] and is publicly available [**AlephData**]. It consists of the mass squared bin center (*sbin*), the bin size (*dsbin*), the normalised invariant mass squared distribution (*sfm2*), the total errors (*derr*) and their correlations (*corerr*). To make the data comparable to our theoretical calculations we have to give the normalised invariant mass squared distribution (*sfm2*) in form of the total decay ratio $R_\tau$. The data is given as the normalised invariant mass squared distribution $(dN_i/ds)/N_i$ scaled by a factor 100 and further normalised to the corresponding branching ratio $i \in$ {V,A,V+A}. Thus we can connect the branching ratio of the i-channel to *sfm2* as follows

$$\mathcal{B}_{V/A} \equiv \int_0^{s_\tau} ds \frac{\text{sfm2}_{V/A}(s)}{100} \equiv \int_0^{s_\tau} ds \mathcal{B}_{V/A} \left( \frac{dN_{V/A}}{N_{V/A}\, ds} \right) \tag{3.4.3}$$

where we used $s_\tau \equiv m_\tau^2$. The total decay ratio $R_\tau$ is defined as the decay width of $\tau$ decaying into hadrons over $\tau$ decaying into electrons. It and can be expressed via the corresponding branching ratios, which can be connected to the invariant mass squared distribution sfm2

$$R_{\tau,V/A} = \frac{\mathcal{B}_{V/A}}{\mathcal{B}_\rceil} = \int_0^{s_\tau} ds \frac{\text{sfm2}_{V/A}(s)}{100\mathcal{B}_e}. \tag{3.4.4}$$

Theoretically the decay ratio is given in **??**. If we neglect the longitudinal contribution $\operatorname{Im}\Pi^{(0)}(s)$ and remember the definition of the spectral function (**??**) and the kinematic weight (**??**), we can write the decay ratio as

$$R_{\tau,i} = \int_0^{s_\tau} \frac{ds}{s_\tau} \omega_\tau(s)\rho(s) \tag{3.4.5}$$

and thus relate the spectral function to the experimental data

$$\rho(s) = \frac{s_\tau}{12\pi^2 100\mathcal{B}_e} \frac{\text{sfm2}}{\omega_\tau}. \tag{3.4.6}$$

To fit the experimental data we define a so-called *spectral function moment* (or *moment*)

$$I_i^{\exp,\omega} \equiv \int_0^{s_0} \frac{ds}{s_0} \omega\left(\frac{s}{s_0}\right) \rho(s), \tag{3.4.7}$$

which will be used in our $\chi^2$ fits, explained in the upcoming section. The data is given for discrete bins so we have to express the integral of the spectral function moment as sum over those bins. The final expression we use to fit parameters to the experimental data is then given by

$$I^{\omega}_{\exp,V/A}(s_0) = \frac{s_\tau}{100\mathcal{B}_e s_0} \sum_{i=1}^{N(s_0)} \frac{\omega\left(\frac{s_i}{s_0}\right)}{\omega_\tau\left(\frac{s_i}{s_\tau}\right)} \mathrm{sfm2}_{V/A}(s_i). \tag{3.4.8}$$

## 3.5 The Method of Least Squares

We apply *method of least squares* (LS) to fit the parameters $\vec{\alpha}$ from the experimental data. Our $\chi^2$-function can be expressed as

$$\chi^2 = \left(I_i^{\exp} - I_i^{\mathrm{th}}(\vec{\alpha})\right) C_{ij}^{\exp-1} \left(I_j^{\exp} - I_j^{\mathrm{th}}(\vec{\alpha})\right), \tag{3.5.1}$$

where $I^{\exp}$/ $I^{\mathrm{th}}$ is a vector of experimental moments/ theoretical moments with the same weight, but different energy cutoffs $s_0$, labelled by the index $i$. In addition $C^{\exp}$ is the covariance matrix describing the correlation of the different experimental moments $C_{ij}^{\exp} = \mathrm{cov}[I_i^{\exp} I_j^{\exp}]$, which is can be computed by the given correlation matrix of the ALEPH data.

In general we aim to minimise the value of $\chi^2$, which will fix the parameter vector $\vec{\alpha}$. The properties of the $\chi^2$-function are well known and the best fits are characterised through $\chi^2/\mathrm{dof} \approx 1$, where the DOF of the fit can be calculated through

$$\mathrm{DOF} = \text{experimental moments} - \text{parameters}. \tag{3.5.2}$$

E.g. if we want to fit $\alpha_s$ and the dimension four Wilson coefficient $C_4$ we get $7 - 2 = 5$ DOF.

For our purposes we use the numerical minimisation computer program MINUIT, which was originally written in FORTRAN by Fred James in the 1970

[**James1975**]. Today in its second version the program has been ported to C++ by the ROOT [**Brun1997**] project at CERN.

The parameter vector $\vec{\alpha}$ includes the strong coupling $\alpha_s$, but also the included OPE Wilson coefficient. Consequently we should have at least as many, if not more moments as parameters we want to fit. As the moments for different $s_0$ are highly correlated we are limited to fit a set of only a few parameters.

It is also possible to increase the number of moments used by using multiple weights $\omega$. Unfortunately using different weights leads to highly correlated moments, which leads to numerical complications by inverting the covariance matrix in **??**. To handle the high correlations we have to redefine our fit quality.

### 3.5.1 Block Diagonal "Fit-Quality"

For fits including multiple weights, which we do not perform in this work,we can redefine LS [**Boito2014**] to

$$Q^2 = \sum_{\omega} \sum_{s_0^i, s_0^j} \left( I_\omega^{exp}(s_0^i) - I_\omega^{th}(s_0^i, \vec{\alpha}) \right) \widetilde{C}^{-1}_{ij,\omega} \left( I_\omega^{exp}(s_0^j) - I_\omega^{th}(s_0^j, \vec{\alpha}) \right), \qquad (3.5.3)$$

where the covariance matrix $\widetilde{C}$ is now a diagonal of the experimental covariance matrices $C_\omega^{exp}$ for each weight

$$\widetilde{C} = \begin{pmatrix} C^{exp}_{\omega=1} & 0 & \dots & 0 \\ 0 & C^{exp}_{\omega=2} & \ddots & \vdots \\ \vdots & \ddots & \ddots & 0 \\ 0 & \dots & 0 & C^{exp}_{\omega=n} \end{pmatrix}. \qquad (3.5.4)$$

As a result we are still able to invert the newly defined covariance matrix $\widetilde{C}$, but minimisation routines like CERN MINUIT are not able to calculate the proper errors for the parameters we want to extract. We have to perform our own error propagation to obtain meaningful errors for the parameters. The error propagation has been derived in [**Boito2011a**, **Boito2011**] and is given as

$$\langle \delta\alpha_k \alpha_l \rangle = A^{-1}_{km} A^{-1}_{ln} \frac{\partial I_i^{th}(\vec{\alpha})}{\partial \alpha_m} \frac{\partial I_r^{th}(\vec{\alpha})}{\partial \alpha_n} \widetilde{C}^{-1}_{ij} \widetilde{C}^{-1}_{ij} \langle \delta I_k^{exp} \delta I_l^{exp} \rangle, \qquad (3.5.5)$$

where

$$A_{kl} = \frac{\partial I^{th}(\vec{\alpha})}{\partial \alpha_k} C^{-1}_{ij} \frac{I^{th}_j(\vec{\alpha})}{\alpha_l}. \qquad (3.5.6)$$

CHAPTER 4

# Measuring the strong coupling

Table 4.1: Timeline

| | |
|---|---|
| 1991 | [**Braaten1991**]: Systematic description, including NP corrections to extract $\alpha_s$ from $R_\tau$. |
| 1992 | [**LeDiberder1992**]: Introducing weights and fit methodology |
| 1993 | [**Aleph1993**] ALEPH measures the strong coupling constant $\alpha_s$ |
| 1998 | [**Opal1998**] OPAL measures the strong coupling constant $\alpha_s$ |
| 2005 | [**Aleph2005**] ALEPH improves their data |
| 2011 | [**Boito2011a**, **Boito2010**]: Include DV. Discover inconsistencies in ALEPH data. |
| 2014 | [**Aleph2014**] ALEPH updates their data. |

The strong coupling has been measured since many years from hadronic $\tau$ decays. An overview of the recently, but different, $\alpha_s$ values can be seen in **??**. Until today most of the applied QCDSR to $\tau$ decays are based on the methodology developed in the early nineties by Braaten, Pich and Narison [**Braaten1991**]. They gathered the at this time available perturbative and NP contributions to extract the strong coupling from comparing their theoretical results to the known inclusive hadronic $\tau$ decay ratio $R_\tau$. Pich together with Le Diberger then formulated the fitting strategy of fitting multiple moments of different weights to extract $\alpha_s$ parallel to Wilson coefficients of the OPE [**LeDiberger1992**], which later has been applied as standard in the ALEPH [**Aleph1993**] as well as the OPAL [**Opal1998**] detectors. For the next ten year years the methodology of extracting the strong coupling did not expe-

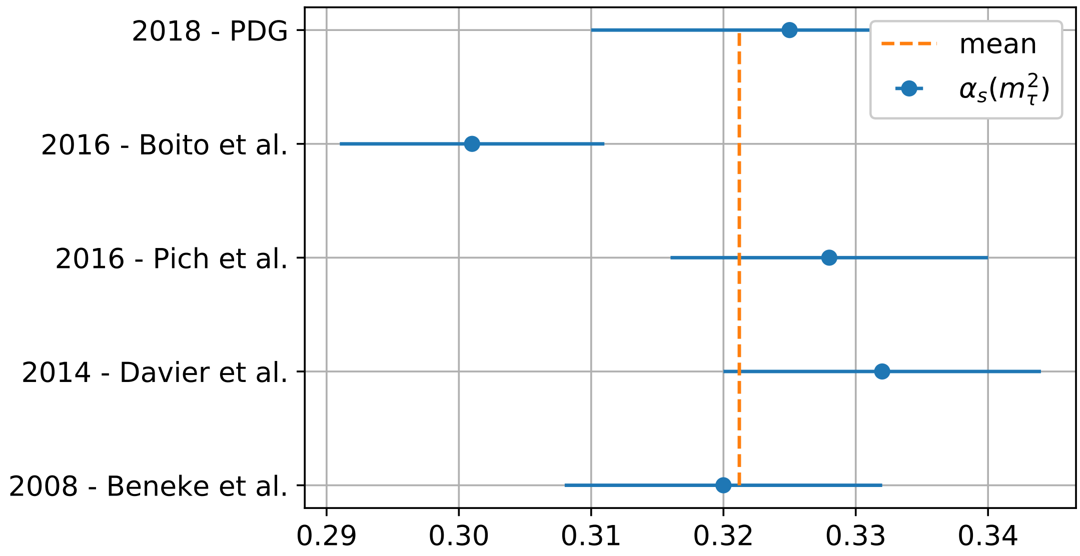


Figure 4.1: Recent values for $\alpha_s(m_\tau^2)$ from hadronic $\tau$ decays. The values are taken from [**PDG2018**, **Boito2016**, **Pich2016**, **Davier2014**, **Beneke2008**], from top to bottom.

rience any major changes until in the year 2011 when Boito, Cata, Golterman, Jamin, Osborn and Peris [**Boito2011a**] applied a duality model to include known DV effects to the QCD analysis of $\tau$ decays. The group around Boito and Pich have different opinions on the importance of the newly introduced duality model [**Pich2016**, **Boito2016**] and consequently we want to deliver a third, opinion on the subject, favouring fits without the duality model.

## 4.1 Fit Strategy

The objective of this work is to extract $\alpha_s$ and argue about the importance of DV. Apart from the two main objectives we want to analyse the contribution of higher order OPE contributions up to dimension ten.

Our fitting strategy will be in choosing weights of lower and higher pinching. Lower pinched weights should be affected by DV, while higher pinched weights should be protected from DV. As a result in comparing different fits of lower and higher pinched weights it should be possible to argue about strength of the DV that are (or are not) present.

| | Symbol | Term | Expansion | OPE Contributions |
|---|---|---|---|---|
| Pinched | $\omega_\tau$ | $(1-x)^2(1+2x)$ | $1-3x^2+2x^3$ | D6, D8 |
| | $\omega_{\text{cube}}$ | $(1-x)^3(1+3x)$ | $1-6x^2+8x^3-3x^4$ | D6, D8, D10 |
| | $\omega_{\text{quartic}}$ | $(1-x)^4(1+3x)$ | $1-10x^2+20x^3-15x^4+4x^5$ | D6, D8, D10, D12 |
| Monomial | $\omega_{M2}$ | $1-x^2$ | $1-x^2$ | D6 |
| | $\omega_{M3}$ | $1-x^3$ | $1-x^3$ | D8 |
| | $\omega_{M4}$ | $1-x^4$ | $1-x^4$ | D10 |
| Pinched $+x$ | $\omega_{X1}$ | $(1-x)$ | $1-x$ | D4 |
| | $\omega_{X2}$ | $(1-x)^2$ | $1-2x+x^2$ | D4, D6 |
| | $\omega_{X3}$ | $(1-x)^3$ | $1-3x+3x^2-x^3$ | D4, D6, D8 |
| | $\omega_{X4}$ | $(1-x)^4$ | $1-4x+6x^2-4x^3+x^4$ | D4, D6, D8, D10 |

Table 4.2: Displaying three categories of fits, each containing three weights with their corresponding mathematical expression and the OPE contributions the fitted integral momentum will be sensitive to.

Our hypothesis is that DV are small enough for fits of the combined vector and axial-vector channel in combination with pinched weights. Consequently we can extract parameters, like the strong coupling $\alpha_s$ from $\tau$ decays to high precision without a DV model.

We will perform our analysis in the framework of FOPT. To define a fit we have to choose a weight $\omega$ and a momentum $s_0$. The only restriction from choosing a weight is, that the weight has to be analytic, leaving us with a variety of choices. For our strategy we have chosen three categories of weights, each of them containing fits with three or four different weights. A table with an overview of all used weights is given in **??** To test for the stability of the fitted values and have enough DOF to fit the higher OPE contributions we furthermore fit every weight for various momenta $s_0$.

## 4.2 Fits

In the following we will give the results of each of the three previously mentioned fit categories.

The first category contains the *Pinched Weights without Monomial x*. The chosen weights are double ($\omega_\tau$), triple ($\omega_{\text{cube}}$) and quadruple ($\omega_{\text{quartic}}$) pinched and do not contain a monomial term $x$. An $x$ term would make the fits sensitive to the $D = 4$ OPE contribution, which causes an unreliable perturbative expansion [**Beneke2012**]. The higher the pinching, the higher the suppression of DV. Consequently if we obtain stable values for $\alpha_s$ from the different pinched fits we should expect the DV to have no influence on the value of the strong coupling. The different weights imply an increasing number of active OPE contributions $D_6, D_8, D_{10}$ and $D_{12}$, which can be used to compare to the stability of higher order OPE contributions and to test for the convergence of the OPE.

The second category contains the *Single Pinched Monomial weights*. In this case all of the weights are only single pinched and, as in the first category, do not carry a monomial in $x$. Consequently if DV affect the fits we should notice different fitting results in comparison to the fits of the first category. Furthermore the single pinched moments only carry two parameters, the strong coupling and an OPE Wilson coefficients. Thus we can further compare the $C_6, C_8$ and $C_{10}$ Wilson coefficients and argue about the stability of the fits.

The third and last category contains a similar pinching as the first category, but this time contains a monomial term in $x$. Consequently these fits are unreliable in the framework of FOPT and we have to apply the *Borel sum* (BS). Following the logic of the second and first category we then can compare the result to analyse the role of DV and compare the Wilson coefficients.

### 4.2.1 Pinched Weights without a Monomial $x$

**Kinematic weight:** $\omega_\tau(x) \equiv (1-x)^2(1+2x)$

We previously encountered the kinematic weight in **??**. It is a polynomial weight function, defined as $\omega_\tau(x) = (1-x)^2(1+2x)$, double pinched, contains the unity and does not contain a term proportional to $x$. Consequently it is an optimal weight [**Beneke2012**]. As a doubled pinched weight it should have a good suppression of DV contributions and its polynomial contains terms proportional to $x^2$ and $x^3$, which makes it sensitive to the dimension six and eight OPE contributions. The fits have been performed within the framework of

| | $s_{min}$ | $\#s_0s$ | $\alpha_s(m_\tau^2)$ | $C_6$ | $C_8$ | $\chi^2/\mathrm{dof}$ |
|---|---|---|---|---|---|---|
| BS | 2.200 | 7 | 0.3274(42) | -0.82(21) | -1.08(40) | 0.21 |
| FOPT | 2.100 | 8 | 0.3256(38) | -0.43(15) | -0.25(28) | 1.30 |
| | 2.200 | 7 | 0.3308(44) | -0.72(20) | -0.85(38) | 0.19 |
| | 2.300 | 6 | 0.3304(52) | -0.69(25) | -0.80(50) | 0.25 |
| | 2.400 | 5 | 0.3339(70) | -0.91(39) | -1.29(83) | 0.10 |
| | 2.600 | 4 | 0.3398(15) | -1.3(1.0) | -2.3(2.5) | 0.01 |

Table 4.3: Table of our fitting values of $\alpha_s(m_\tau^2), C_6$ and $C_8$ for the kinematic weight $\omega(x) = (1-x)^2(1+2x)$ using FOPT ordered by increasing $s_{min}$. The errors are given in parenthesis after the observed value.

FOPT for different numbers of $s_0$. The momentum sets are characterised by its lowest energy $s_{min}$. We fitted values down to 1.5 GeV. Going to lower energies is questionable due to the coupling constant becoming large, which implies a breakdown of PT. Furthermore it bares the risk to be affected by the $\rho(770)$ and $a_1$ peaks in the vector and axial-vector spectral function, which we cannot model within the framework of the OPE. For the three fitting parameters $\alpha_s, C_6$ and $C_8$ we have given the results in **??** and graphically in **??**.

We only display the fits for $s_{min}$ larger than 2.1 GeV. We noted a jump between the $s_{min} = 2.1$ GeV and $s_{min} = 2.2$ GeV of the $\chi^2/\mathrm{dof}$ from 0.19 to 1.3. We consequently discarded fits with a $s_{min} < 2.2$ GeV, as fits lower $s_{min}$ behave more stable[1]. The values for the less momenta are preferred by us due to two reasons. First below energies of 2.2 GeV we have to face the problematic influence of increasing resonances. Second, we will see, that the values obtained from the lower moment fits are more compatible with our other fits series. We further discarded the fit with four $s_0$s momenta, which has very small $\chi^2/\mathrm{dof} = 0.01$. This is due to the fact, that we have four $s_0$s momenta to fit three parameters, which leaves us with too few DOF.

The selected fits with 8-10 momenta have a small $\chi^2$ per DOF. The fitted parameters, $\alpha_s, c_6$ and $c_8$ are in good agreement with each other. For all fits we have a good convergence of the OPE. For later comparisons we will give the means

[1] As will be seen by comparing the kinematic weight with the cubic and quartic weight

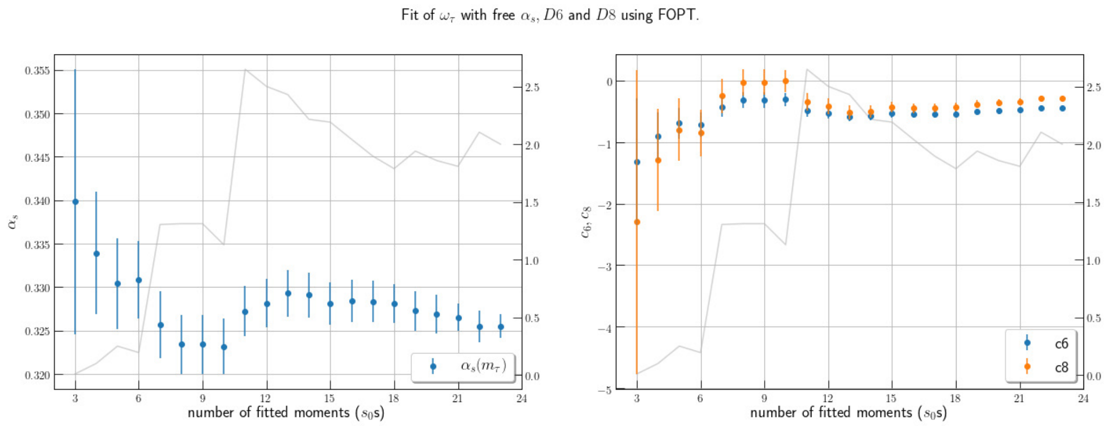


Figure 4.2: Fitting values of $\alpha_s(m_\tau^2)$, $C_6$ and $C_8$ for the kinematic weight $\omega(x) = (1-x)^2(1+2x)$ using FOPT for different $s_{min}$. The left graph plots $\alpha_s(m_\tau^2)$ for different numbers of used $s_0$s. The right plot contains the dimension six and eight contributions to the OPE. Both plots have in grey the $\chi^2$ per DOF.

for the strong coupling, $D = 6$ and $D = 8$ contributions:

$$\alpha_s(m_\tau^2) = 0.3317(33), \quad C_6 = -0.77(17) \quad \text{and} \quad C_8 = -0.98(35). \tag{4.2.1}$$

We further tested the stability of the dimension six and eight contributions to the OPE within the same fit series but for a fixed value of the strong coupling to our previous averaged result $\alpha_s(m_\tau^2) = 0.3179$. The values for $C_6$ and $C_8$ are larger than the values given in our final results from **??**. This is explained with a smaller contribution from the strong coupling, which has to be compensated by larger OPE contributions.

Additionally we applied the BS for the fit below the $\chi^2$ threshold containing seven $s_0$s. Even though we used a different framework than FOPT the results are compatible. This further underlines the good results of the kinematic weight fit and can be seen as an indicator for FOPT being the superior framework as compared to CIPT.

**Cubic weight:** $\omega_{cube}(x) \equiv (1-x)^3(1+3x)$

To further consolidate the results from the kinematic weight, we tested a weight of higher pinching, which should suppress DV more than a double pinched weight. Consequently, if we obtain similar results to our previous fits we could exclude DV effects for the kinematic weight. On the other hand,

| $s_{min}$ | $\#s_0s$ | $\alpha_s(m_\tau^2)$ | $C_6$ | $C_8$ | $C_{10}$ | $\chi^2/dof$ |
|---|---|---|---|---|---|---|
| 2.000 | 9 | 0.3228(26) | -0.196(27) | 0.075(28) | 0.420(56) | 1.96 |
| 2.100 | 8 | 0.3302(40) | -0.52(11) | -0.58(22) | -1.00(45) | 0.43 |
| 2.200 | 7 | 0.3312(43) | -0.56(12) | -0.68(23) | -1.23(50) | 0.55 |
| 2.300 | 6 | 0.336(11) | -0.78(47) | -1.17(98) | -2.38(22) | 0.29 |
| 2.400 | 5 | 0.3330(96) | -0.63(47) | -0.82(10) | -1.51(26) | 0.48 |

Table 4.4: Table of our fitting values of $\alpha_s(m_\tau^2), C_6, C_8$ and $C_{10}$ for the cubic weight $\omega(x) = (1-x)^3(1+3x)$ using FOPT ordered by increasing $s_{min}$. The errors are given in parenthesis after the observed value.

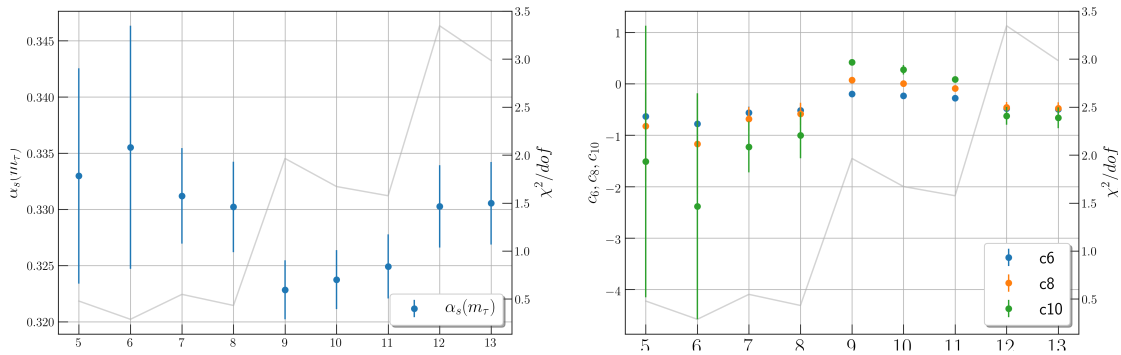


Figure 4.3: Graphic representation of the fitting values of $\alpha_s(m_\tau^2)$ in the left and $C_6, C_8$ and $C_{10}$ in the right plot for the cubic weight $\omega(x) = (1-x)^3(1+3x)$. The fits have been performed in the FOPT scheme and the data points are given with error bars and are ordered by increasing $s_{min}$. The grey line in displays the $\chi^2$ function.

any differences to the previous fit would indicate present DV in the kinematic weight. Our *cubic* weight will be triple pinched and optimal, as it does not contain a $x$ monomial. It is due to its polynomial structure sensitive to the dimensions six, eight and ten contributions of the OPE, which yields one more parameter to fit than with the kinematic weight $\omega_\tau$. The fitting results can be seen in **??** and graphically in **??**.

As before we performed fits for $s_0 \leqslant 1.5\,\text{GeV}$, but could only reach convergence for fits with energies larger or equal than $1.8\,\text{GeV}$. As before the $\chi^2$ makes a jump at $s_0 = 2.1\,\text{GeV}$ to values per DOF of almost 2. Consequently we excluded theses fits and focused on fits from five to eight $s_0$s momenta.

The selected fits have a good $\chi^2/\mathrm{dof}$ and the fitted parameters, $\alpha_s, C_6, C_8$ and $C_{10}$ are in agreement with each other, except for the fit with six momenta. The fit with a $s_{min} = 2.3\,\mathrm{GeV}$ has the lowest $\chi^2 = 0.29$ and error on $\alpha_s$, but takes slighlty different values for the OPE Wilson coefficients in comparison to the other selected fits. The means for the strong coupling, $D = 6$ and $D = 8$ contributions:

$$\alpha_s(m_\tau^2) = 0.33, \quad C_6 = -0.62, \quad C_8 = -0.81 \quad \text{and} \quad C_{10} = -1.5. \tag{4.2.2}$$

We furthermore found that the OPE is converging, but not as fast as for the kinematic weight. The values of $\left|\delta^{(8)}\right|$ is only half as large as $\left|\delta^{(8)}\right|$. The values of the lower momentum count are in high agreement with the ones obtained from the kinematic weight. The conclusions that we take from the *cubic weight* are that the kinematic weight, with its double pinching, should sufficiently suppress any contributions from DVs. If DV would have an effect on the kinematic weight, we should have seen an improvement of the fits with the *cubic* weight, due to its triple pinching, which is not the case.

**Quartic weight:** $\omega(x) \equiv (1-x)^4(1+4x)$

The last fits of the the pinched weights without a monomial term in $x$ uses the *quartic weight* defined as $\omega(x) \equiv (1-x)^4(1+4x)$. It contains five fitting parameters ($\alpha_s, C_6, C_8, C_{10}, C_{12}$) and did only converge for $s_{min} = 2\,\mathrm{GeV}$ (nine $s_0$s momenta). The results for , with a $\chi^2$ per DOF of 0.67 are given by:

$$\begin{aligned} &\alpha_s(m_\tau^2) = 0.3290(11), \quad C_6 = -0.3030(46), \quad C_8 = -0.1874(28), \\ &\quad C_{10} = 0.3678(45) \quad \text{and} \quad C_{12} = -0.4071(77) \end{aligned} \tag{4.2.3}$$

Due to the problematic of the fitting routing, which is caused by too many OPE contributions fitted simultaneously, we will discard the fitting results for the quartic weight.

### 4.2.2 Single Pinched Monomial Weights

To further solidate our hypothesis we want to probe some weights with a single pinching. If DV play a role then we should note deviating results to fits with higher pinchings. The advantage of these weights is that they only let

| $s_{min}$ | $\#s_0s$ | $\alpha_s(m_\tau^2)$ | $C_6$ | $\chi^2/\text{dof}$ |
|---|---|---|---|---|
| 2.100 | 8 | 0.3179(47) | -0.42(17) | 1.62 |
| 2.200 | 7 | 0.3248(52) | -0.77(22) | 0.38 |
| 2.300 | 6 | 0.3260(60) | -0.85(28) | 0.43 |

Table 4.5: Table of our fitting values of $\alpha_s(m_\tau^2)$, and $C_6$ for the single pinched double power monomial weight $\omega_{M2}(x) = 1 - x^2$ using FOPT ordered by increasing $s_{min}$. The errors are given in parenthesis after the observed value.

one OPE dimension contribute, thus leaving us with only two parameters per fit.

#### Second power monomial: $\omega_{M2}(x) \equiv 1 - x^2$

The first weight is defined as $\omega_{M2}(x) \equiv 1 - x^2$. We only have to fit two parameters, the strong coupling $\alpha_s$ and the dimension six OPE contribution. The results can be seen in **??**. Like in the $\omega_\tau$ and $\omega_{cubic}$ we obtain stable fits for $s_{min} \leqslant 2.2\,\text{GeV}$, but the $\chi^2/\text{dof}$ jumps to values $\chi^2/\text{dof} > 1.6$ for smaller $s_{min}$. The values obtained for fitting six and seven $s_0s$ moments are in good agreement with each other and furthermore carry a acceptable $\chi^2$ per DOF. The averaged values for both parameters are

$$\alpha_s(m_\tau^2) = 0.3254(40) \qquad \text{and} \qquad C_6 = -0.81(18) \tag{4.2.4}$$

We note that the strong coupling obtained from the single pinched weight is similar to the one of the previous fits ($\approx 3.33$) which indicates, that even single pinched weights have sufficiently suppressed DV.

#### Third power monomial: $\omega_{M3}(x) \equiv 1 - x^3$

The second weight is defined as $\omega_{M3}(x) \equiv 1 - x^3$ and contains a single third power monomial. Consequently it is sensitive to dimension eight contributions from the OPE. Our fitting results can be taken from **??**. Due to the good $\chi^2$ and the internally compatible fitting values we averaged over all rows except the last one of **??**. The last row, at $s_{min} = 2.8\,\text{GeV}$ has only one DOF and

| $s_{min}$ | $\#s_0s$ | $\alpha_s(m_\tau^2)$ | $C_8$ | $\chi^2/\text{dof}$ |
|---|---|---|---|---|
| 2.100 | 8 | 0.3147(44) | -0.27(29) | 1.71 |
| 2.200 | 7 | 0.3214(49) | -1.01(39) | 0.41 |
| 2.300 | 6 | 0.3227(57) | -1.18(54) | 0.46 |
| 2.400 | 5 | 0.3257(67) | -1.58(74) | 0.39 |
| 2.600 | 4 | 0.325(10) | -1.54(1.53) | 0.58 |
| 2.800 | 3 | 0.326(21) | -1.69(4.03) | 1.17 |

Table 4.6: Table of our fitting values of $\alpha_s(m_\tau^2)$, and $C_8$ for the single pinched third power monomial weight $\omega_{M3}(x) = 1 - x^3$ using FOPT ordered by increasing $s_{min}$. The errors are given in parenthesis after the observed value.

| $s_{min}$ | $\#s_0s$ | $\alpha_s(m_\tau^2)$ | $C_{10}$ | $\chi^2/\text{dof}$ |
|---|---|---|---|---|
| 2.100 | 8 | 0.3136(43) | -0.07(54) | 1.75 |
| 2.200 | 7 | 0.3203(48) | -1.64(77) | 0.42 |
| 2.300 | 6 | 0.3216(56) | -2.01(1.13) | 0.47 |
| 2.400 | 5 | 0.3247(66) | -2.98(1.62) | 0.39 |
| 2.600 | 4 | 0.324(10) | -2.86(3.69) | 0.58 |
| 2.800 | 3 | 0.325(20) | -3.43(10.74) | 1.17 |

Table 4.7: Table of our fitting values of $\alpha_s(m_\tau^2)$ and $C_{10}$ for the single pinched fourth power monomial weight $\omega_{M4}(x) = 1 - x^4$ using FOPT ordered by increasing $s_{min}$. The errors are given in parenthesis after the observed value.

consequently high errors. The averaged values are given by

$$\alpha(m_\tau^2) = 0.32382(42) \qquad \text{and} \qquad C_8 = -1.33(67). \tag{4.2.5}$$

**Fourth power monomial:** $\omega_{M4}(x) \equiv 1 - x^4$

We already analysed the cubic and quartic weights, which depend on the dimension ten OPE contribution, in **??** and **??** correspondingly. Now, even with the visible DV for fourth power monomial $\omega_{M4} \equiv 1 - x^4$ to study another single pinched moment and the dimension ten OPE contribution. The results of the are given in **??**. The fitting behaviour is very similar to the third power monomial (**??**) and we will directly cite our obtained results:

$$\alpha_s(m_\tau^2) = 0.32277(40) \qquad \text{and} \qquad C_{10} = -2.4(3.6). \tag{4.2.6}$$

The values for the strong coupling are a little bit lower than the ones obtained by the kinematic and cubic weight fits. Furthermore the error on the tenth dimension contribution of the OPE are large. All in all the usage of the single pinched fourth power monomial weight is questionable and does not deliver any additional insights.

### 4.2.3 Pinched Weights with monomial $x$

Next to the previously mentioned *optimal weights* from Beneke and Jamin [**Beneke2012**] there exist another type of *optimal′ weights*[2] introduced by Pich [**LeDiberder1992**]

$$\omega_{(n,m)}(x) = (1-x)^n \sum_{k=0}^{m} (k+1)x^k, \tag{4.2.7}$$

Combinations of these optimal moments have been widely used by the ALEPH collaboration to perform QCD analysis on the LEP data. The moments fitted in this section include the for FOPT problematic proportional term in $x$, thus we will perform additional fits using the Borel-sum.

$$\omega_{X1} \equiv (1-x)$$

The first weight is single pinched with only two fitting parameters: $\alpha_s$ and $\chi^2/\mathtt{dof}$. The results for BS and FOPT fits have been displayed in **??**. We note that the $\alpha_s$ values of the two frameworks differ, which is most probably due to the problematic of the monomial in $x$, appearing in the weight function. In general we trust the results of the BS more than those of FOPT. This is further underlined while regarding the higher $\chi^2/\mathtt{dof}$ values of the FOPT fits. Moreover the values of the BS fits agree with each other, whereas the fits of the FOPT yield inconsistent values. Regarding explicitly the fits from the BS we note that the fits have good $\chi^2/\mathtt{dof}$ values, although a jump from 0.2 to 0.95 between the first two fitted moments. Also note that we had to fit the invariant gluon-

[2] Pich has a different definition of "optimal" moments than Beneke and Jamin. To differentiate the two definition we marked Pich's optimal′ moments with an apostrophe.

| | $s_{min}$ | $\#s_0 s$ | $\alpha_s(m_\tau^2)$ | $\langle aGG\rangle_I$ | $\chi^2/\mathrm{dof}$ |
|---|---|---|---|---|---|
| BS | 2.100 | 8 | 0.357(12) | -0.072(23) | 0.95 |
| | 2.200 | 7 | 0.3593(97) | -0.079(19) | 0.2 |
| | 2.300 | 6 | 0.3589(99) | -0.078(20) | 0.24 |
| FOPT | 2.100 | 8 | 0.3176(47) | -0.0134(48) | 1.62 |
| | 2.200 | 7 | 0.3246(52) | -0.2262(59) | 1.91 |
| | 2.300 | 6 | 0.3260(60) | -0.2453(73) | 1.71 |

Table 4.8: Table of our fitting values of $\alpha_s(m_\tau^2)$ and $langleaGG\rangle_I$ for the single pinched optimal weight $\omega_{X1}(x) = (1-x)$ using the FOPT and BS ordered by increasing $s_{min}$. The errors are given in parenthesis after the observed value.

condensate for the first time. In the literature $\langle aGG\rangle_I$ should be around 2.1, but here we obtain a smaller, negative value, which could be connected to problems in the fit.

$$\omega_{X2} \equiv (1-x)^2$$

The next weight is double pinched. Additionally to the strong coupling and the invariant gluon-condensate we also had to fit the dimension six OPE contribution. Our fits can be seen in **??**. If we compare the BS with the FOPT fits we note, next to the before mentioned incompatibilities, a sign difference for the $D = 6$ contribution. From now we will skip the FOPT discussion for weights containing a monomial $x$ term, and trust in the BS fits. In comparison to the previous fit with the single pinched weight we have higher $\chi^2/\mathrm{dof}$ values, a lower $\alpha_s$ value and an $\langle aGG\rangle_I$ numeric value similar to the value from the literature around $0.21$, but with opposite sign. Consequently we note some tension between the single pinched weight and the double pinched weight, which could be caused by DV being not sufficiently suppressed by a single pinched weight containing a monomial $x$.

| | $s_{min}$ | $\#s_0s$ | $\alpha_s(m_\tau^2)$ | $\langle aGG\rangle_I$ | $C_6$ | $\chi^2/\text{dof}$ |
|---|---|---|---|---|---|---|
| BS | 2.100 | 8 | 0.3207(48) | -0.0170(50) | -0.45(17) | 1.90 |
| | 2.200 | 7 | 0.3270(54) | -0.0254(61) | -0.77(21) | 0.74 |
| | 2.300 | 6 | 0.3253(63) | -0.0232(75) | -0.69(27) | 0.9 |
| FOPT | 2.100 | 8 | 0.3331(54) | -0.0108(45) | 0.361(76) | 1.9 |
| | 2.200 | 7 | 0.3401(57) | -0.0185(52) | 0.220(88) | 0.73 |
| | 2.300 | 6 | 0.3383(68) | -0.0165(67) | 0.26(12) | 0.89 |

Table 4.9: Table of our fitting values of $\alpha_s(m_\tau^2), \langle aGG\rangle_I$ and $C_6$ for the double pinched optimal weight $\omega_{X2}(x) = (1-x)^2$ using the BD or FOPT ordered by increasing $s_{min}$. The errors are given in parenthesis after the observed value.

| | $s_{min}$ | $\#s_0s$ | $\alpha_s(m_\tau^2)$ | $\langle aGG\rangle_I$ | $C_6$ | $C_8$ | $\chi^2/\text{dof}$ |
|---|---|---|---|---|---|---|---|
| BS | 2.000 | 9 | 0.3169(20) | -0.0123(34) | -0.29(12) | -0.05(24) | 2.0 |
| | 2.100 | 8 | 0.3239(40) | -0.0212(42) | -0.63(15) | -0.74(29) | 0.46 |
| | 2.200 | 7 | 0.3251(17) | -0.02283(56) | -0.689(12) | -0.879(33) | 0.56 |
| FOPT | 2.000 | 9 | 0.33985(81) | -0.01124(43) | 0.002(10) | -0.242(26) | 1.59 |
| | 2.100 | 8 | 0.3480(47) | -0.0201(36) | -0.264(89) | -1.03(28) | 0.31 |
| | 2.200 | 7 | 0.3483(23) | -0.0204(41) | -0.27(15) | -1.05(40) | 0.41 |

Table 4.10: Table of our fitting values of $\alpha_s(m_\tau^2), \langle aGG\rangle_I, C_6$ and $C_8$ for the optimal weight $\omega_{X3}(x) = (1-x)^3$ using the BS or FOPT ordered by increasing $s_{min}$. The errors are given in parenthesis after the observed value.

$$\omega_{X3} \equiv (1-x)^3 \textbf{ and } \omega_{X4} \equiv (1-x)^4$$

The fits with a triple and quadruple pinched weight do not give any further insights. We give the results in **??** and **??**. Both of the weights include similar values to the double pinched weights, which affirms problems with the single pinched weight of this category. The quadruple pinched weight contains five fitting parameters and as a result has notable convergence problems.

| | $s_{min}$ | $\#s_0s$ | $\alpha_s(m_\tau^2)$ | aGGInv | $C_6$ | $C_8$ | $C_{10}$ | $\chi^2/dof$ |
|---|---|---|---|---|---|---|---|---|
| BS | 1.950 | 10 | 0.31711(67) | -0.012432(24) | -0.30013(73) | -0.06785(16) | 0.26104(50) | 1.09 |
| | 2.000 | 9 | 0.3206(24) | -0.0167(14) | -0.455(38) | -0.373(67) | -0.36(14) | 0.83 |
| | 2.100 | 8 | 0.3248(21) | -0.02230(47) | -0.6724(63) | -0.834(14) | -1.352(28) | 0.23 |
| FOPT | 1.950 | 10 | 0.3416(14) | -0.01306(83) | -0.050(22) | -0.390(59) | -0.50(19) | 1.71 |
| | 2.100 | 8 | 0.3480(25) | -0.0201(27) | -0.264(91) | -1.02(23) | -339.00(20) | 0.41 |

Table 4.11: Table of our fitting values of $\alpha_s(m_\tau^2)$, $\langle aGG \rangle_I$, $C_6$, $C_8$ and $C_{10}$ for the optimal weight $\omega_{X4}(x) = (1-x)^4$ using the BS or FOPT ordered by increasing $s_{min}$. The errors are given in parenthesis after the observed value.

| | weight | $s_{min}$ | $\alpha_s(m_\tau^2)$ | $\langle aGG \rangle_I$ | $C_6$ | $C_8$ | $C_{10}$ | $\chi^2/dof$ |
|---|---|---|---|---|---|---|---|---|
| FOPT | $\omega_\tau$ | 2.2 | 0.3308(44) | - | -0.72(20) | -0.85(38) | - | 0.19 |
| | $\omega_{cube}$ | 2.1 | 0.3302(40) | - | -0.52(11) | -0.58(22) | -1.00(45) | 0.43 |
| | $\omega_{M2}$ | 2.2 | 0.3248(52) | - | -0.77(22) | - | - | 0.38 |
| | $\omega_{M3}$ | 2.2 | 0.3214(49) | - | - | -1.01(39) | - | 0.41 |
| BS | $\omega_{X2}$ | 2.2 | 0.3270(54) | -0.0254(61) | -0.77(21) | - | - | 0.74 |
| | $\omega_{X3}$ | 2.1 | 0.3239(40) | -0.0212(42) | -0.63(15) | -0.74(29) | - | 0.46 |

Table 4.12: Table of the best fits. The fits have been selected as being closest to the previously discussed $\chi^2/dof$ jump. Each weight includes the strong coupling $\alpha_s(m_\tau^2)$ as a fitting variable. The first four fits have been performed using FOPT and the last two have been performed using BS. They are visually distinguished in the table by a horizontal line.

## 4.3 Comparison

To create an overview of our previous results we have gathered the most compatible rows by hand. The fits have been selected by regarding the $\chi^2/dof$ threshold. For every weight, which is we did not mark problematic, we have chosen a fit closest, but below the $\chi^2/dof$ threshold. They are shown in **??**, which is composed of two parts. The upper four rows are fits using FOPT and the lower two rows are fits using BS. The fits are in great agreement with each others. The strong coupling as the OPE contributions up to dimension eight are compatible within small error ranges. We have visualised the different values and errors in **??** to underline their agreement. The fits furthermore all have a

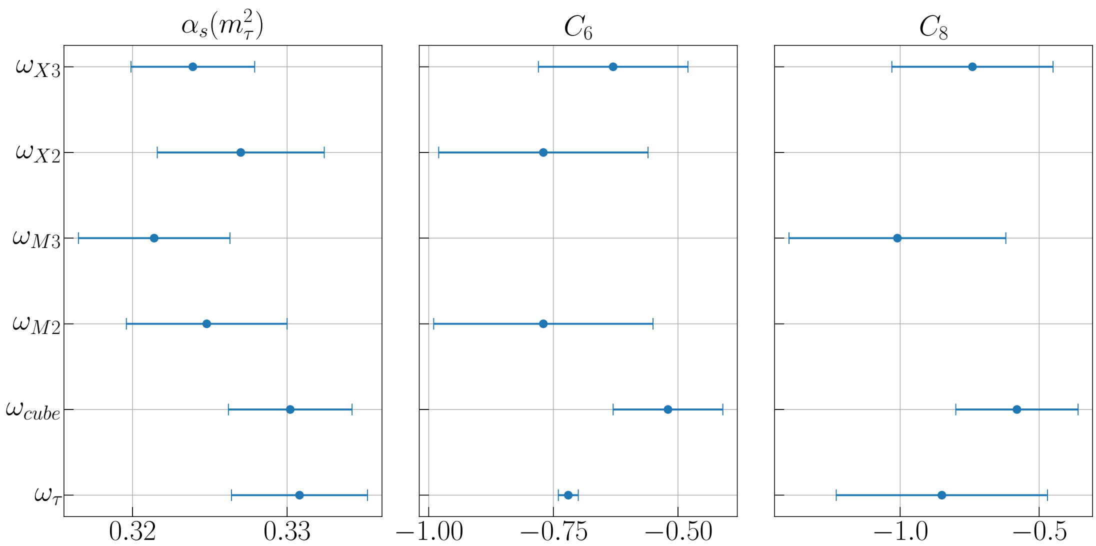


Figure 4.4: dies das

good $\chi^2/\mathrm{dof}$.

As the weights $\omega_{M2}$ and $\omega_{M3}$ are only single pinched, but still in high agreement with the other higher pinched weights we conclude that DV only play a minor role, even for single pinched weights!

As a result for $\alpha_s$ we state the outcome of the $\omega_\tau$ fit. The kinematic weight is double pinched, does not contain a monomial $x$ term and has only three parameters to fit. The final value $\alpha_s$ then reads

$$\alpha_s(m_\tau^2) = 0.3308 \pm 0.0044. \tag{4.3.1}$$

The dimension six OPE contribution is very stable. Stating the result from the kinetic weight fit yields

$$C_6 = -0.72 \pm 0.2. \tag{4.3.2}$$

Note that the $C_6$ values from the cubic weight are slightly different. This is due to the fact, that the cubic weight includes a fourth fitting parameter, which contribution needs to be compensated by the other parameters.

The value of higher dimension OPE parameters are still compatible, but have a higher variation than the previous two parameters. Beginning from the $D = 10$ contribution we do not have enough good fits to evaluate their contribution.

Consequently we do not state a single value for OPE parameters of dimension eight and higher.

Chapter 5

# Conclusions

We have performed a QCD analysis on hadronic $\tau$ decays to determine a value of $\alpha_s$ at the $m_\tau^2$ scale without including DV. We have excluded DV to contrast the previous analysis of Boito et al., which stated the necessity of incorporating a model describing DV. To argument we employed a new set of weights to probe the suppression of DV.

The the strong coupling we obtained at the $m_\tau^2$ scale from our fits is

$$\alpha_s(m_\tau^2) = 0.3308(44). \tag{5.0.1}$$

Running this value to the $m_z$ scale yields

$$\alpha_s(m_Z) = 0.1200, \tag{5.0.2}$$

which is around 0.002 larger than the $\tau$ decay and general average taken from **[PDG2018]**.

For DV we found that in the framework of FOPT in the V+A channel no additional model is needed for double pinched weights. Even for single pinched weights we obtained stable results.

We also performed fits using the BS, yielding comparable results to the values obtained from FOPT. In the debate of FOPT vs CIPT we interpret this outcome in favour of the former and discourage the usage of CIPT.

Chapter 6

# Constants

In **??** we collect all used constants that we have used in performing our fits.

| Quantity | Value | Reference |
|---|---|---|
| $V_{ud}$ | $0.9742 \pm 0.00021$ | ? |
| $S_{EW}$ | $1.0198 \pm 0.0006$ | ? |
| $B_e$ | $17.815 \pm 0.023$ | ? |
| $m_\tau$ | 1.77686 error? | ? |
| $\langle aGG \rangle_I$ | $0.012\,\mathrm{GeV}^2$ | ? |
| $\langle \overline{q}_{u/d} q_{u/d} \rangle_I$ | $-0.020\,123\,648\,\mathrm{MeV}$ | ? |
| $\langle \overline{q}_s q_s \rangle_I$ | $-0.016\,098\,918\,4\,\mathrm{MeV}$ | ? |

Table 6.1: Numerical values of used constants in our fitting routine.

Chapter 7

# Coefficients

## 7.1 β function

There are several conventions for defining the $\beta$ coefficients, depending on a minus sign and/or a factor of two (if one substitues $\mu \to \mu^2$) in the $\beta$-function **??**. We follow the convention from Pascual and Tarrach (except for the minus sign) and have taken the values from [**Boito2011**]

$$\beta_1 = \frac{1}{6}(11N_c - 2N_f), \tag{7.1.1}$$

$$\beta_2 = \frac{1}{12}(17N_c^2 - 5N_cN_f - 3C_fN_f), \tag{7.1.2}$$

$$\beta_3 = \frac{1}{32}\left(\frac{2857}{54}N_c^3 - \frac{1415}{54}N_c^2N_f + \frac{79}{54}N_cN_f^2 - \frac{205}{18}N_cC_fN_f + \frac{11}{9}C_fN_f^2 + C_f^2N_f\right), \tag{7.1.3}$$

$$\beta_4 = \frac{140599}{2304} + \frac{445}{16}\zeta_3, \tag{7.1.4}$$

where we used $N_f = 3$ and $N_c = 3$ for $\beta_4$.

## 7.2 Anomalous mass dimension

$$\gamma_1 = \frac{3}{2}C_f, \tag{7.2.1}$$

$$\gamma_2 = \frac{C_f}{48}(97N_c + 9C_f - 10N_f), \tag{7.2.2}$$

$$\gamma_3 = \frac{C_f}{32}\left[\frac{11413}{108}N_c^2 - \frac{129}{4}N_c C_f - \left(\frac{278}{27} + 24\zeta_3\right)N_c N_f + \frac{129}{2}C_f^2 - (23 - 24\zeta_3)C_f N_f - \frac{35}{27}N_f^2\right], \tag{7.2.3}$$

$$\gamma_4 = \frac{2977517}{20736} - \frac{9295}{216}\zeta_3 + \frac{135}{8}\zeta_4 - \frac{125}{6}\zeta_5, \tag{7.2.4}$$

where $N_c$ is the number of colours, $N_f$ the number of flavours and $C_f = (N_c^2 - 1)/2N_c$. We fixed furthermore fixed $N_f = 3$ and $N_c = 3$ for $\gamma_4$.

## 7.3 Adler function

# List of Abbreviations

NPT Non-Perturbative Theory, page 7

NP Non-Perturbative, page 7

OPE Operator Product Expansion, page 18

PT Perturbative Theory, page 7

QCD Quantum Chromodynamics, page 4

QFT Quantum Field Theory, page 3

RGE Renormalisation Group Equation, page 9

SM Standard Model, page 3

CHPT Chiral Perturbation Theory, page 7

LQCD Lattice Quantum Chromodynamics, page 8

QCDSR Quantum Chromodynamics Sum Rules, page 8